THE JOURNAL OF BIOLOGICAL CHEMISTRY VOL. 286, NO. 11, pp. 9443–9456, March 18, 2011

Ubiquitin-dependent Proteasomal Degradation of Human Liver Cytochrome P450 2E1

IDENTIFICATION OF SITES TARGETED FOR PHOSPHORYLATION AND UBIQUITINATION[*][S]

Received for publication, August 19, 2010, and in revised form, December 6, 2010 Published, JBC Papers in Press, January 5, 2011, DOI 10.1074/jbc.M110.176685

YongQiang Wang[‡], Shenheng Guan[§], Poulomi Acharya[‡], Dennis R. Koop[¶], Yi Liu[‡], Mingxiang Liao[‡], Alma L. Burlingame[§], and Maria Almira Correia[‡§‖1]**

*From the Departments of [‡]Cellular and Molecular Pharmacology, [§]Pharmaceutical Chemistry, and [‖]Bioengineering and Therapeutic Sciences and **The Liver Center, University of California, San Francisco, California 94158-2517 and the [¶]Department of Physiology and Pharmacology, Oregon Health and Science University, Portland, Oregon 97239-3098*

Human liver CYP2E1 is a monotopic, endoplasmic reticulum-anchored cytochrome P450 responsible for the biotransformation of clinically relevant drugs, low molecular weight xenobiotics, carcinogens, and endogenous ketones. CYP2E1 substrate complexation converts it into a stable slow-turnover species degraded largely via autophagic lysosomal degradation. Substrate decomplexation/withdrawal results in a fast turnover CYP2E1 species, putatively generated through its futile oxidative cycling, that incurs endoplasmic reticulum-associated ubiquitin-dependent proteasomal degradation (UPD). CYP2E1 thus exhibits biphasic turnover in the mammalian liver. We now show upon heterologous expression of human CYP2E1 in *Saccharomyces cerevisiae* that its autophagic lysosomal degradation and UPD pathways are evolutionarily conserved, even though its potential for futile catalytic cycling is low due to its sluggish catalytic activity in yeast. This suggested that other factors (*i.e.* post-translational modifications or "degrons") contribute to its UPD. Indeed, in cultured human hepatocytes, CYP2E1 is detectably ubiquitinated, and this is enhanced on its mechanism-based inactivation. Studies in Ubc7p and Ubc5p genetically deficient yeast strains *versus* corresponding isogenic wild types identified these ubiquitin-conjugating E2 enzymes as relevant to CYP2E1 UPD. Consistent with this, *in vitro* functional reconstitution analyses revealed that mammalian UBC7/gp78 and UbcH5a/CHIP E2-E3 ubiquitin ligases were capable of ubiquitinating CYP2E1, a process enhanced by protein kinase (PK) A and/or PKC inclusion. Inhibition of PKA or PKC blocked intracellular CYP2E1 ubiquitination and turnover. Here, through mass spectrometric analyses, we identify some CYP2E1 phosphorylation/ubiquitination sites in spatially associated clusters. We propose that these CYP2E1 phosphorylation clusters may serve to engage each E2-E3 ubiquitination complex *in vitro* and intracellularly.

Hepatic cytochromes P450 (P450s)[2] are endoplasmic reticulum (ER)-anchored hemoproteins involved in the metabolism of numerous endo- and xenobiotics. These substrates can modulate P450 content, diversity, and/or function (see Refs. 1, 2 and references therein) through induction via either increased synthesis or protein stabilization, *i.e.* half-life prolongation (3–9). By contrast, "suicide" substrate/inactivators accelerate the degradation of certain P450s and dramatically curtail their half-lives (10–23). Such substrate-mediated P450 induction and/or enhanced turnover can influence the severity and the time course of certain pharmacokinetic/pharmacodynamic drug-drug interactions and is an important therapeutic consideration (24–27).

P450 turnover has been proposed to involve various proteolytic mechanisms (6–9, 28–38). However, it is now increasingly evident that in common with other type I monotopic ER proteins, P450s such as CYPs 3A (both native and structurally inactivated) undergo ER-associated degradation (ERAD) involving the ubiquitin (Ub)-dependent 26 S proteasomal system (UPS) (6–9, 12–16). This process entails the ubiquitination of the predominantly cytosol (C)-localized monotopic ER proteins by an E2 Ub-conjugating enzyme (Ubc)-E3 Ub ligase complex, its concurrent extraction from the ER membrane by the p97-AAA ATPase, and its delivery to the 26 S proteasome (12–17, 39, 40). CYPs 3A thus may qualify as typical ERAD-C substrates. On the other hand, P450s such as CYPs 2B1 and 2C11 undergo autophagic lysosomal degradation (ALD) (32–36). Yet others such as CYP2E1 apparently involve both UPD and ALD (18–22, 37, 38). Accordingly, the rat liver CYP2E1 undergoes biphasic degradation with a rapid phase ($t_{1/2}$, 7 h) and a slow phase ($t_{1/2}$, 37 h) that reflect its degradation via ERAD/UPS and ALD, respectively. The rapid phase is thought to stem from structural damage inflicted by its futile oxidative cycling either in the absence or on withdrawal of an appropriate substrate (*i.e.* EtOH). Thus,

* This work was supported, in whole or in part, by National Institutes of Health Grants GM44037 (to M. A. C.), DK26506 (to M. A. C.), and NCRRRR 01614 (to A. L. B.).

[S] The on-line version of this article (available at http://www.jbc.org) contains supplemental Figs. S1–S6 and data 1–3.

[1] To whom correspondence should be addressed: Dept. of Cellular and Molecular Pharmacology, University of California, San Francisco, Mission Bay Campus, Genentech Hall, N572F/Box 2280/5th Floor, 600 16th St., San Francisco, CA 94158-2517. Tel.: 415-476-3992; Fax: 415-476-5292; E-mail: almira.correia@ucsf.edu.

[2] The abbreviations used are: P450, cytochrome P450; ALD, autophagic-lysosomal degradation; b_5, cytochrome b_5; BisIII, bisindolylmaleimide III; CHIP, C terminus of Hsc70-interacting protein; CuOOH, cumene hydroperoxide; CZ, chlorzoxazone; DDEP, 3,5-dicarbethoxy-2,6-trimethyl-4-ethyl-1,4-dihydropyridine; ER, endoplasmic reticulum; ERAD, ER-associated degradation; HRD, genes involved in HMG-CoA reductase degradation; HMM, high molecular mass; Lys-C, lysylendopeptidase C; IB, immunoblotting; OR, NADPH-P450 oxidoreductase; Ub, ubiquitin; UBC, genes for Ub-conjugating enzymes; UPD, Ub-dependent proteasomal degradation; UPS, Ub-dependent 26 S proteasomal system; 6-OHZ, 6-hydroxychlorzoxazone.

substrate binding stabilizes the CYP2E1 protein and prolongs its half-life, channeling it into the slower ALD pathway. Furthermore, abolition of the redox electron flux through functional inactivation of NADPH-cytochrome P450 oxidoreductase (OR) stabilizes CYP2E1 and prolongs its half-life, consistent with its reduced futile oxidative cycling (41, 42).

To determine the extent to which CYP2E1 catalytic turnover influences the particular route of its degradation, we used *Saccharomyces cerevisiae* not only because of its high evolutionary conservation of the eukaryotic ERAD/UPS/ALD pathways (43–45) but also because its relatively poor constitutive OR content (46) would sustain virtually little basal CYP2E1 catalytic turnover. Thus, if CYP2E1 UPD were largely dependent on its futile catalytic turnover, we reasoned that the ALD pathway of CYP2E1 turnover should predominate in these yeast cells. We therefore examined the turnover of heterologously expressed human CYP2E1 in *S. cerevisiae* strains with genetically defined functional defects in the 19 S Hrd2p/Rpn1 proteasomal subunit (*hrd2-1*), genetic deletion of the vacuolar (lysosomal) master protease Pep4p (*pep4*Δ), as well as corresponding isogenic wild type (WT) strains. Our findings revealed that despite the overall sluggish CYP2EI catalytic turnover in yeast, its degradation was still dependent on both ERAD/UPS and ALD as in the mammalian liver.

Similar turnover analyses of heterologously expressed CYP2E1 in *S. cerevisiae* strains (*ubc4*Δ, *ubc4*Δ/*ubc5*Δ, *ubc7*Δ, and *ubc6*Δ/*ubc7*Δ) with specific genetic deletions of the known ERAD-associated E2s Ubc4p, Ubc5p, Ubc6p, and/or Ubc7p (43–45) indicated that Ubc5p and Ubc7p were important for CYP2E1 ERAD.

The above findings in yeast were fully consistent with a significant contribution of both ERAD/UPS and ALD to its *in vivo* turnover in cultured human hepatocytes. In these hepatocytes, CYP2E1 was appreciably ubiquitinated, and this ubiquitination was greatly enhanced after proteasomal inhibition, which stabilized the enzyme. Cotreatment with the ALD inhibitors 3-methyladenine (3MA) and NH_4Cl also stabilized CYP2E1.

The involvement of Ubc5p in yeast CYP2E1 ERAD is consistent with the reported involvement of its mammalian UbcH5a E2 counterpart in CYP2E1 ubiquitination by CHIP (C terminus of Hsp70-interacting protein), a cytosolic E3 Ub ligase (22). The involvement of Ubc7p suggested that a UBC7-dependent mammalian Ub ligase could also be involved in CYP2E1 ubiquitination. One such E3 candidate is gp78/AMFR (autocrine motility factor receptor), an ER integral protein (47) that is involved in CYP3A4 ubiquitination (48–50). Our findings described below indicate that both UbcH5a-CHIP and UBC7-gp78 E2-E3 complexes can ubiquitinate CYP2E1 *in vitro*. As in the case of UBC7/gp78-mediated CYP3A4 ubiquitination (48), protein kinase (PK) A- and/or PKC-mediated phosphorylation also enhanced UBC7/gp78-mediated CYP2E1 ubiquitination. We now document that such protein phosphorylation also enhances UbcH5a/CHIP-mediated ubiquitination of CYP2E1. Furthermore, inhibition of PKA or PKC with a specific inhibitor (KT-5720 or bisindolylmaleimide (BisIII)) or a general inhibitor (staurosporine) blocked both CYP2E1 ubiquitination and turnover in cultured hepatocytes, thereby underscoring the physiological relevance of CYP2E1 protein phosphorylation to its ERAD/UPD.

Using LC-MS/MS analyses, we have identified several CYP2E1 residues, in addition to the previously identified Ser^{129} (28, 51–53) specifically phosphorylated by PKA or PKC in the native enzyme. Furthermore, we document that this phosphorylation is further enhanced after CYP2E1 structural inactivation by cumene hydroperoxide (CuOOH).[3] Not only is the overall extent of CYP2E1 phosphorylation increased, but additional residues also are targeted for PKA/PKC-mediated phosphorylation. Additionally, using LC-MS/MS analyses, we have also identified some CYP2E1 Lys residues ubiquitinated by the UbcH5a/CHIP- and UBC7/gp78-mediated systems.

EXPERIMENTAL PROCEDURES

Materials—Media for yeast growth were purchased from Clontech. Calpain inhibitor I was purchased from Calbiochem, and okadaic acid was obtained from Invitrogen. The sources of many chemicals have been previously reported (40, 48–50). Benzyloxycarbonyl-Leu-Leu-Leu-$B(OH)_2$ (MG262) and epoxomycin were purchased from Boston Biochem (Boston, MA). Nickel-nitrilotriacetic acid superflow resin was obtained from Qiagen (Valencia, CA), and ceramic hydroxyapatite multimodal chromatography media were from Bio-Rad. γ-*S*-[^{32}P]ATP (specific activity, 6000 Ci/mmol) was obtained from PerkinElmer Life Sciences. Goat polyclonal IgGs against a recombinant CYP3A4 enzyme and sheep polyclonal IgGs against CYP2E1 (54) were raised commercially and partially purified by ammonium sulfate fractionation.

Rat brain PKC (catalytic subunit) was obtained from Calbiochem-Novabiochem, and recombinant PKA (catalytic subunit) was from New England Biolabs (Ipswich, MA). Endoproteinase Lys-C (sequencing grade) was from Roche Applied Science. Ub-activating enzyme E1 was purchased from Biomol (Plymouth Meeting, PA). Human cytosolic C-terminal gp78 (E3) and murine UBC7 (E2) were expressed in *Escherichia coli* and purified as described previously (49), respectively, from plasmid pGEX-gp78C encoding the human cytosolic C-terminal gp78 domain (residues 309–643) and pGEX-MmUBC7 encoding murine UBC7. Both plasmids were gifts from Dr. A. M. Weissman. Chaperones Hsp70, Hsc70, and Hsp40 were purchased from Assay Designs (Ann Arbor, MI). Ub-conjugating enzyme E2 UbcH5a was obtained from Boston Biochem. Plasmid pET-CHIP-His_6 encoding the full-length 303-residue human CHIP as a His-tagged fusion inserted in-frame into pET-30a vector was provided by Dr. Cam Patterson and was described previously (49). Recombinant cytochrome b_5 (b_5) and OR were expressed in *E. coli* and purified as detailed (55). All other buffers and reagents were of the highest commercial grade.

Expression and Purification of CYP2E1-His_6—A cDNA encoding a C-terminally His_6-tagged human CYP2E1 (kindly

[3] CuOOH at the concentrations used directly inactivates P450 enzymes resulting in oxidative fragmentation of their prosthetic heme to mono- and dipyrrolic products that covalently bind the protein at the active site and irreversibly modify the enzyme, similarly to that observed after DDEP-mediated mechanism-based inactivation of CYP3A (12, 99).

provided by Dr. Todd Porter, University of Kentucky, Lexington) was incorporated into a pCWori vector and expressed in DH5α cells, grown in TB media at 37 °C with isopropyl β-D-thiogalactopyranoside induction. The temperature was lowered to 30 °C, and the cells were allowed to grow for 20 h, with periodic monitoring of spectral P450 content to determine maximal P450 expression. Recombinant CYP2E1 was purified to homogeneity by nickel affinity chromatography, followed by detergent exchange by hydroxylapatite chromatography as described previously (48). Aliquots of the purified protein were stored at −80 °C until use. Rabbit liver CYP2E1 was purified as described previously (56).

Yeast Expression, Cell Growth, Harvest, and Microsomal Preparation for CYP2E1 Degradation Analyses—Isogenic yeast strains were generated as described previously (43–45). Briefly, expression vectors pYES2-ADH-CYC (modified from pYES2/CT, *URA*-marked, and under control of *ADH1* instead of the *GAL1* promoter) and pYcDE-2 (*TRP*-marked, under the control of the yeast *ADH1* promoter) were employed for insertion of a wild type human CYP2E1 cDNA to yield pYES2-ADH-2E1 and pYcDE-ADH-2E1, respectively. The yeast strains used have been described previously (35, 36, 39, 45). The conditions for yeast cell transformation and culture growth have been described previously (35, 36, 39, 45, 48). In brief, yeast strains transformed with CYP2E1 expression vector were grown at 30 °C in a synthetic defined medium with appropriate supplements, as specifically indicated. Cells were harvested at an early culture stage during the logarithmic growth phase of the culture (*A* of ≈0.8–1.0 at 600 nm) or at an intermediate stage after "stationary chase" generally 12 h after reaching an *A* of 0.5–0.8 at 600 nm. For *pep4*Δ and *hrd2-1* yeast strains, an extra harvesting time point was added at an even later stage after stationary chase, generally 20–24 h after reaching an *A* of 0.5 at 600 nm.

Yeast microsomal fractions were prepared exactly as described previously (35, 36, 39). The microsomal pellet was overlaid with potassium phosphate buffer, pH 7.4, containing 1 mM DTT, 0.1 mM EDTA, and 20% (v/v) glycerol and stored at −80 °C until used.

Western immunoblotting analyses of CYP2E1 proteins were carried out with yeast microsomes against sheep polyclonal anti-CYP2E1 IgGs. After methanol/H_2SO_4 precipitation and acetone washes of yeast microsomes to eliminate interference in the protein assay from variable amounts of adventitious chromophoric material, the protein content was determined. Yeast microsomal protein (30 μg) was subjected to SDS-PAGE and then transferred electrophoretically to a nitrocellulose membrane. Sheep anti-CYP2E1 IgG was used as the primary antibody (1:10,000, v/v) with rabbit anti-sheep horseradish peroxidase-coupled antibody as the secondary (1:40,000, v/v), and a Pierce Femto ECL detection system to assay immunochemically detectable CYP2E1 content. The immunoblots were densitometrically quantitated using ImageJ software, and the results were statistically analyzed by the Student's *t* test.

Chlorzoxazone (CZ) 6-Hydroxylase Activity—WT *S. cerevisiae* was transformed with pYES2-ADH-2E1 (or pYcDE-ADH-2E1) as described above and harvested at an early culture stage during the logarithmic growth phase of the culture (*A* of ≈0.8–1.0 at 600 nm) before degradation begins. Microsomes were prepared as described above, and aliquots containing 100 pmol of spectrally monitored CYP2E1 hemoprotein were used either before or after functional reconstitution with OR (OR/P450 molar ratios 4:1) and b_5 (b_5/P450 molar ratios 2:1), by incubating OR and b_5 with yeast microsomal suspensions on ice for 30 min (57). Hepes buffer (50 mM), pH 7.4, CZ (200 μM), and an NADPH-generating system were then added, and after a 3-min preincubation at 37 °C, the reaction was initiated with isocitrate dehydrogenase and incubated for 30 min (54, 57). In parallel, a positive control of acetone-treated rabbit liver microsomal incubation was included. An aliquot of these microsomes with 2500 pmol of 6-OHCZ added was also incubated in parallel as the positive recovery control for the extraction and analysis. The 6-OHCZ was quantified by HPLC analyses with 7-OH coumarin as the internal standard as described previously (54, 57).

Human Hepatocyte Culture, DDEP Treatment, and CYP2E1 Degradation Analyses—Human hepatocytes (3.2–3.5 million) from four different human donors were cultured on a collagen type I substratum with a Matrigel overlay as detailed (58–60). Cells were maintained for 2 days with a daily change of medium, and then CYP2E1 was induced with rifampin (10 μM) for 3 days. Treatments were carried out on the 5th day of culture. Cells were treated with vehicle (ethanol or DMSO) and proteasomal inhibitor MG-262 (20 μM), MG-132 (20 μM), or epoxomycin (10 μM), with or without DDEP (100 μM) for 0–6 h. Hepatocytes from another human donor were also similarly cultured and treated with rifampin. On the 5th day they were treated with a combination of lysosomal inhibitors 3-methyladenine (3MA; 5 mM) and NH_4Cl (50 mM) for 20 h, along with a DMSO vehicle control (16). Total cell lysate protein (20 μg) was assayed by Western immunoblotting for CYP2E1 content as described above.

CYP2E1 Ubiquitination Analyses—Total lysate proteins (300 μg) in a final concentration of 2% w/v SDS and 5 mM *N*-ethylmaleimide were heated at 95 °C for 5 min. Total CYP2E1 was immunoprecipitated with sheep anti-CYP2E1 IgG (1 mg) cross-linked to protein A-Sepharose CL-4B after the mixture was rotated end-to-end at 4 °C overnight. The immunoprecipitated CYP2E1 was solubilized with SDS-PAGE loading buffer (50 μl) containing 5% w/v SDS, 20% v/v glycerol, 50 mM DTT, and 5% v/v β-mercaptoethanol in 50 mM Tris buffer, pH 6.8, and boiled for 5 min, and the equivalent aliquots (48 μl) were subjected to SDS-PAGE on 4–20% Tris-HCl gels and transferred to a nitrocellulose membrane, followed by rabbit anti-Ub IgG as the primary antibody (Sigma; 1:100, v/v), goat anti-rabbit horseradish peroxidase-coupled secondary antibody (Bio-Rad, 1:40,000, v/v), with a Pierce Femto ECL detection system employed to detect CYP2E1 ubiquitination.

In Vitro Reconstitution Assays of CYP2E1 Ubiquitination—Purified recombinant human CYP2E1-His_6 was inactivated for 15 min at 37 °C with 1 mM CuOOH, 1 mM EDTA, 1 mM GSH in 50 mM Hepes buffer, pH 7.4, containing 10% v/v glycerol. DTT (5 mM) was added to quench CuOOH at the end of the reaction. CuOOH-inactivated CYP2E1 (250 pmol) was then incubated in either reconstituted UbcH5a/CHIP or UBC7/gp78 ubiquitination systems as described previously (48, 49).

For analysis of its UbcH5a/CHIP-mediated ubiquitination, CYP2E1 was CuOOH-inactivated in the presence of Hsc70 (2.5

μM) and Hsp40 (2.5 μM), and then added to a reconstituted system consisting of E1 (0.1 μM), UbcH5a (1.5 μM), CHIP-His_6 (4 μM), Hsc70 (2.5 μM) and Hsp40 (2.5 μM), ATP (5 mM), creatine phosphokinase (20 units), creatinine phosphate (20 mM), $MgCl_2$ (12 mM), ^{32}P-Ub (167 μM; prepared as detailed in Ref. 49), Hepes buffer (50 mM, pH 7.4, containing 20% v/v glycerol), EGTA (0.5 mM), EDTA (0.5 mM), with or without PKA (0.004 units), and/or PKC (0.004 units) addition in a final volume of 70 μl. Control reactions were incubated in parallel for 90 min in the absence of ATP or CYP2E1.

The UBC7/gp78 ubiquitination system was similarly reconstituted with E1 (0.68 μM), human UBC7 (4.25 μM), and purified recombinant gp78C (the cytosolic 63-kDa E3 ligase domain; 1 μM). The other components were the same as described above, except that Hsp70/Hsp40 was omitted. Control reactions were incubated in parallel for 90 min in the absence of ATP or CYP2E1, and CuOOH-inactivated CYP3A4 was also included in parallel as a positive control (48, 49).

All reactions were incubated at 30 °C for 90 min. At the end of each reaction, *N*-ethylmaleimide (5 mM, final concentration) was added followed by 10% w/v SDS to a final concentration of 2%, and the samples were boiled for 5 min. CYP2E1 was immunoprecipitated with sheep anti-CYP2E1 IgG (1.5 mg) cross-linked to protein A-Sepharose CL-4B (100 μl) after the mixture was rotated end-to-end at 4 °C overnight essentially as described previously. The immunoprecipitated CYP2E1 was solubilized with 50 μl of SDS-PAGE loading buffer (48, 49), and equivalent aliquots (48 μl) were subjected to SDS-PAGE on 4–20% Tris-HCl gels. The gels were dried and exposed to PhosphorImager screens and visualized using a Typhoon scanner. CYP3A4 was immunoprecipitated with goat anti-CYP3A4 IgG and analyzed as detailed (48, 49).

In Vivo Effects of PKA/PKC Inhibitors on CYP2E1 UPD/ERAD in Cultured Rat Hepatocytes—To determine whether PKA/PKC-enhanced CYP2E1 ubiquitination was relevant to its physiological degradation, we examined the effects of a specific PKA and PKC inhibitor, KT-5720 and BisIII, respectively, as well as that of staurosporine, a general PKA/PKC/PKG inhibitor. Rat hepatocytes cultured exactly as described above were pretreated with ethanol (200 mM)/acetone (20 mM) to induce CYP2E1 for 3 days, weaned off these CYP2E1-stabilizing inducers for another day, and then subjected to ^{35}S-pulse-chase analyses on the 5th day (40). Following chase, they were treated with DDEP (100 μM), and 30 min later with vehicle (DMSO), KT-5720 (5 μM), BisIII (5 μM), or staurosporine (1 μM). Cells were harvested at 0, 2, and 4 h following DDEP treatment. CYP2E1 was immunoprecipitated as described above, and aliquots were subjected to radioactive scintillation counting, as well as SDS-PAGE/PhosphorImager analyses and Typhoon scanning as described above.

Mass Spectrometric (MS) Analysis and Protein/Peptide Identification—Protein samples were reduced, alkylated, and subjected to SDS-PAGE separation. Protein bands were excised from the gel, followed by in-gel digestion with lysylendopeptidase C (Lys-C) as detailed previously (48). The peptides were analyzed by LC-MS/MS analyses on LTQ-FT or LTQ Orbitrap mass spectrometer (ThermoFisher Scientific, San Jose, CA), equipped with a Waters NanoAcquity LC system (Milford, MA). Peptides were trapped on a C18 trap column before separation in a 100 μm inner diameter × 100 mm long C18 analytical column, with a linear gradient from 2% solvent A (0.1% formic acid in water) to 35% solvent B (0.1% formic acid in acetonitrile) at 350 nl/min over 35 min. The MS method was a "top 6" data-dependent sequence with one survey scan in FT mode having mass resolution of 30,000 followed by six CID scans in LTQ targeting the first six most intense peptide ions whose m/z values were not in the dynamically updated exclusion list. The MS/MS data were searched against the SwissProt database using the in-house Protein Prospector search engine (61, 62), with a concatenated database consisting of normal and randomized decoy databases (63, 64). False discovery rates for phosphorylation and ubiquitination assays were estimated to be 1 and 5%, corresponding to the expectation values of 0.01 and 0.05, respectively. The retention times of modified peptides provided additional evidence to support the peptide identification and modification site assignment especially for multisite phosphorylated peptides.

Phosphorylation of Native/CuOOH-inactivated CYP2E1 by PKA/PKC—Purified recombinant CYP2E1 was inactivated with CuOOH (CuOOH-inactivated) or without (native CYP2E1). The proteins were then incubated with PKA or PKC (sample incubated without ATP as a control) at 30 °C for 30 min, as described previously (48). At the end of the reaction, the reaction mixture was reduced, alkylated, and subjected to SDS-PAGE, followed by in-gel digestion with Lys-C as described above. For database searches, variable modifications on serine and threonine were allowed. The phosphopeptide identification and the site assignment were manually verified by inspection of the raw MS/MS spectra.

Estimation of PKA/PKC-catalyzed CYP2E1 Phosphorylation Stoichiometry—CYP2E1 phosphorylation stoichiometry was estimated by application of a label-free semi-quantitative analysis, which relies on the extraction of selected ion chromatograms of peptide ions from the survey scan mass spectra, whose peptide identification was obtained from a database search of corresponding MS/MS spectra. Protein/peptide identification, the phosphorylation site assignment, as well as information on the relative stoichiometry can be obtained from two LC-MS/MS experiments with unphosphorylated (control) and phosphorylated (sample) preparations (65, 66).

Identification of CYP2E1 Ubiquitination Sites—Purified human or rabbit liver CYP2E1 (500 pmol) was subjected to *in vitro* ubiquitination for 90 min with either the complete UbcH5a/CHIP or UBC7/gp78 system as detailed above. The reaction was terminated with a 2% w/v SDS (final concentration), and the mixture was boiled for 5 min, followed by reduction through addition of DTT (25 mM), and further incubation at 37 °C for 1 h. Iodoacetamide (75 mM) was then added to alkylate the protein, and the mixture was placed in the dark at room temperature for another hour. This mixture was then diluted at least five times with a buffer consisting of Tris (50 mM, pH 7.4), NaCl (150 mM), EDTA (1 mM), 10% v/v glycerol, and 0.5% Nonidet P-40 before addition of disuccinimidyl suberate cross-linked sheep anti-CYP2E1 IgG-protein A-Sepharose beads (≈500 μg of sheep anti-CYP2E1 IgG; 200 μl) and gently rotated at 4 °C overnight. The beads were extensively washed

with the same buffer and eluted with SDS-PAGE loading buffer (80 μl) as described above. The eluate was boiled for 5 min, and subjected to 4–15% SDS-PAGE analysis followed by staining of the gels with Coomassie Blue. Gel pieces corresponding to a molecular mass range of 55–250 kDa were excised, finely chopped, destained with 50% v/v methanol in 50 mM ammonium bicarbonate, and then dehydrated by addition of acetonitrile. The dried gel pieces were then rehydrated with 50 mM ammonium bicarbonate containing Lys-C/trypsin (side chain protected porcine trypsin; Promega, Madison, WI) in an ≈1:20 w/w ratio of each protease to CYP2E1, placed on ice for 20 min, followed by sufficient 50 mM ammonium bicarbonate to cover the gel pieces. The protein was digested at 37 °C for at least 12 h. The peptides were extracted with 50% acetonitrile, 5% formic acid three times by vortexing and water bath sonication. The extracted peptides were concentrated by speed vacuum and desalted through a C18 ZipTip. They were then subjected to LC-MS/MS analysis as described above. In addition to commonly variable modifications such as methionine oxidation and protein N-terminal acetylation, Gly-Gly (uncleaved Lys), Leu-Arg-Gly-Gly (uncleaved Lys), and phospho (Ser, Thr) modifications were also considered in the database search. Peptides with expectation values of 0.05 or less were accepted. Phosphorylated/ubiquitinated peptides were confirmed by manual inspection of the raw MS/MS spectra (see supplemental material). MS/MS spectra were inspected for the diagnostic loss of GG- or KGG-associated mass (114.043 or 242.1 Da, respectively) that not only verified the Ub-derived protein modification but also served to identify the precise CYP2E1 Lys residue ubiquitinated (67).

RESULTS

Sluggish CYP2E1 Catalytic Function in Yeast Microsomes—The yeast *S. cerevisiae* constitutively expresses relatively low levels of the P450 redox partner OR, thereby accounting for the relatively sluggish catalytic turnover of heterologously expressed mammalian microsomal P450s in the absence of coexpressed OR (46). Indeed, assay of a selective CYP2E1 functional marker CZ 6-hydroxylase in *S. cerevisiae* microsomes containing heterologously expressed human CYP2E1 verified that their basal activity was 5.4% that of the corresponding yeast microsomes functionally reconstituted with exogenous OR and b_5 (Fig. 1). For reference, the positive control of acetone-treated and thus CYP2E1-enriched rabbit liver microsomes included in parallel exhibited an activity of 2553 pmol of 6-OHCZ/mg protein/min. These findings thus indicated that the heterologously expressed CYP2E1 enzyme in yeast microsomes is intrinsically active and competent when functionally reconstituted, albeit at a fraction of the activity of its rabbit liver counterpart. Thus, under basal conditions and in the absence of exogenously supplemented redox partners, the potential of yeast microsomal CYP2E1 for futile oxidative cycling would be relatively low, unlike that of its mammalian liver microsomal counterparts (41, 42).

CYP2E1 Degradation Analyses in S. cerevisiae—Given this low potential for futile oxidative cycling, it was plausible that the relative flux of CYP2E1 into UPD and ALD pathways would be altered in yeast. Human liver CYP2E1 was therefore heterologously expressed in isogenic WT HRD and hrd2-1 (defective in 19 S proteasomal Hrd2p/Rpn1 subunit) yeast strains as well as in PEP4 WT and *pep4*Δ yeast strains (deficient in the vacuolar Pep4p master protease) (Fig. 2). These findings indicated that a fraction of CYP2E1 is initially stabilized to a significant extent in the *hrd2-1* yeast strains relative to the corresponding control WT strains (Fig. 2*A*). However, at a later time, another fraction is also stabilized (≈2-fold) in *pep4*Δ yeast strains (Fig. 2*B*). These findings thus revealed that both UPD and ALD function as the major CYP2E1 proteolytic pathways in yeast, just as in the mammalian liver.

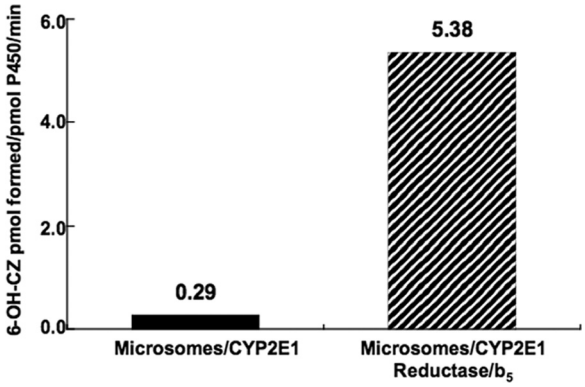

FIGURE 1. **CZ 6-hydroxylase activity of *S. cerevisiae* microsomal membranes after heterologous expression of CYP2E1.** Assays were carried out before and after functional reconstitution of microsomal CYP2E1 with OR and b_5, as described previously (see under "Experimental Procedures"). The corresponding activities per mg of microsomal protein were 15 and 270 pmol of 6-OHCZ/mg protein/min, respectively. A positive control of acetone-treated rabbit liver microsomes yielded an activity of 2553 pmol of 6-OHCZ/mg protein/min, which was 9.5-fold higher than that of the functionally reconstituted yeast microsomes (270 pmol/mg protein/min). Values are averages derived from two separate microsomal incubations.

Relative CYP2E1 Degradation in WT and Ubc5- and Ubc7-deficient Yeast Strains—The Ub-conjugating enzymes UbcH5a and UBC7, identified in *in vitro* P450 ubiquitination systems (22, 49), have corresponding homologs in yeast, and thus yeast strains deficient in these E2 enzymes (*ubc4*Δ, *ubc4*Δ/*ubc5*Δ, *ubc7*Δ, and *ubc6*Δ/*ubc7*Δ) were examined for clues to their specific roles in CYP2E1 ERAD. On heterologous expression, significant stabilization of human liver CYP2E1 was observed *in vivo* in *ubc4*Δ/*ubc5*Δ, *ubc7*Δ, and *ubc6*Δ/*ubc7*Δ yeast strains, relative to their corresponding WT strains (Fig. 3). However no significant CYP2E1 stabilization over that of the WT type was observed in the *ubc4*Δ yeast strain, thereby indicating that Ubc4p enzyme is dispensable to this process. However, when its deletion is combined with that of Ubc5p, the CYP2E1 is greatly stabilized in the *ubc4*Δ/*ubc5*Δ strain (Fig. 3*A*). Comparable CYP2E1 stabilization in *ubc7*Δ and *ubc6*Δ/*ubc7*Δ yeast strains also similarly excluded a significant contribution of Ubc6p E2 enzyme to CYP2E1 ERAD (Fig. 3*B*). Collectively, these findings reveal that Ubc5p and Ubc7p are the most relevant yeast E2 enzymes in CYP2E1 ERAD, consistent with the findings of the *in vitro* reconstituted ubiquitination systems with mammalian E2/E3 proteins (22, 49; see below). The ERAD-associated E3 enzymes were not similarly evaluated in yeast, first because no known homolog of mammalian CHIP exists in yeast; and second, none of the known yeast ERAD E3s appears to participate

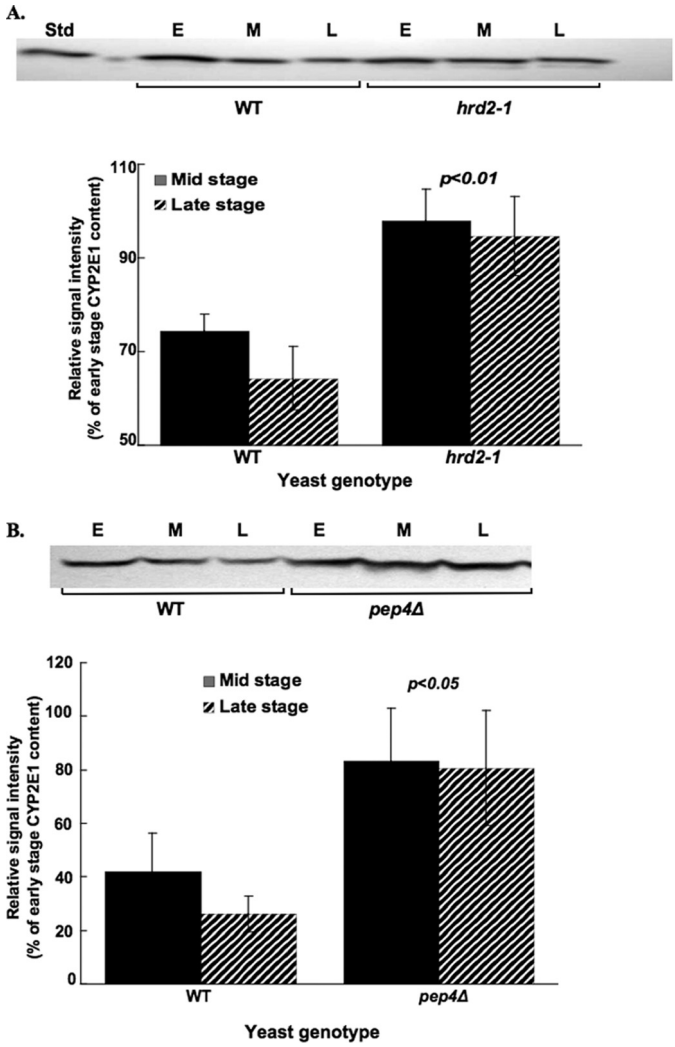

FIGURE 2. **Degradation of heterologously expressed human liver CYP2E1 in yeast with defective proteasomal and deleted vacuolar function.** A plasmid encoding human liver CYP2E1 was heterologously expressed in yeast strains defective in proteasomal degradation (*hrd2-1*) or deficient in vacuolar degradation (*pep4*Δ), and corresponding isogenic wild type (*WT*) yeast strains, and its degradation was followed by the stationary chase method as described previously (46, 50). Yeast cells were harvested at various stages of logarithmic culture growth corresponding to an A_{600} of 0.8 (*E,* early), 12 h after reaching this value (*M,* middle stage), or 20 h after reaching an A_{600} of 0.8 (*L,* late), as required for monitoring ALD in yeast. Microsomes were subjected to IB analyses with sheep anti-CYP2E1 IgG as the primary antibody and rabbit anti-sheep HRP-coupled secondary IgG, followed by ECL detection as described previously (50). Prototypical immunoblots are shown with a purified human liver CYP2E1 standard included as a standard (*Std*). *A,* immunochemically detected CYP2E1 levels at middle and late stages were densitometrically quantitated and expressed as % of the initial "early" stage levels in the WT or the *hrd2-1* strain. Values are mean ± S.D. of three individual yeast cultures. *B,* immunochemically detected CYP2E1 levels at middle and late stages were densitometrically quantitated and expressed as % of the initial early stage levels in the WT or the *pep4*Δ strain. Values are mean ± S.D. of three individual yeast cultures.

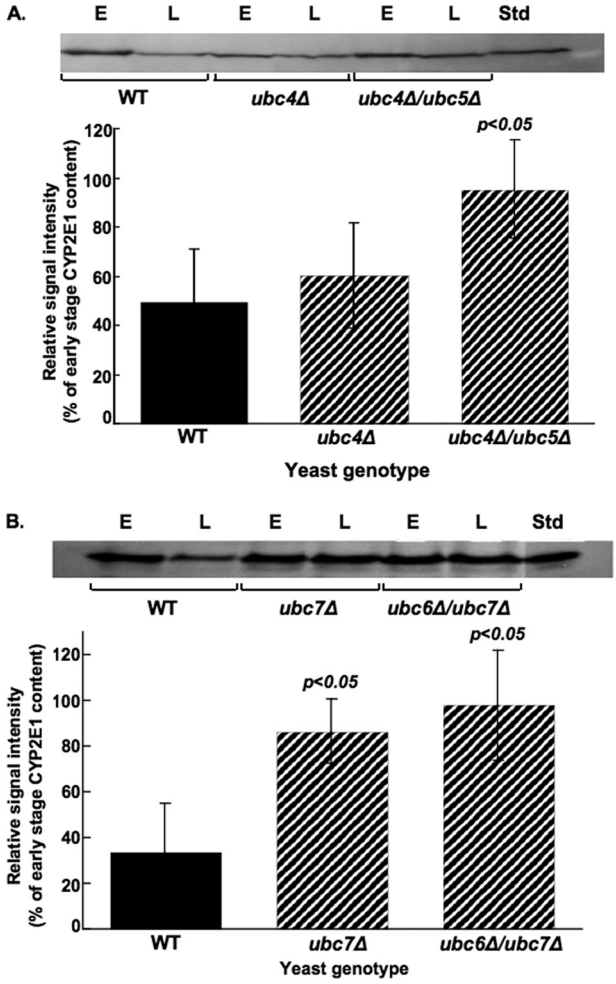

FIGURE 3. **Degradation of heterologously expressed human liver CYP2E1 in yeast with genetic deletions of ERAD-associated E2 enzymes.** CYP2E1 was heterologously expressed in yeast strains deficient in Ubc4p (*ubc4*Δ) or both Ubc4p and Ubc5p (*ubc4*Δ/*ubc5*Δ), and corresponding isogenic WT yeast strains (*A*), or in yeast strains deficient in Ubc7p (*ubc7*Δ) or both Ubc6p and Ubc7p (*ubc6*Δ/*ubc7*Δ) (*B*). Cells were harvested at an absorbance of ≈0.8–1.0 at 600 nm (early stage) or after stationary chase, generally 12 h after reaching an *A* of 0.5–0.8 at 600 nm (middle stage), and CYP2E1 degradation was followed as described previously in Fig. 2 for the HRD and *hrd2-1* strains. Values are mean ± S.D. of three individual yeast cultures. *Std*, standard.

in CYP3A ERAD (50), even though gp78 shares 30% homology to HRD-1 (47, 68, 69).

CYP2E1 UPD in Cultured Human Hepatocytes—To determine the clinical relevance of this process, cultured human hepatocytes were pretreated with the CYP3A/CYP2E1 inducer rifampin (60). Western immunoblotting analyses of the corresponding lysates from cells revealed a small loss of the native ≈50-kDa CYP2E1 parent species over 6 h of culture, reflecting its normal physiological turnover. This loss was inhibited in the presence of the proteasome inhibitor MG262 or epoxomycin (Fig. 4*A*; supplemental Fig. S1). Ubiquitination analyses of CYP2E1 immunoprecipitates from human hepatocyte lysates similarly confirmed significant post-translational modification of the protein *in vivo*, and this ubiquitination was appreciably increased upon MG262 treatment, thereby revealing that a significant fraction of the native CYP2E1 protein was subjected to 26 S proteasomal degradation (Fig. 4*C*). Treatment with the P450 suicide/mechanism-based inactivator DDEP resulted in a marked loss of the parent ≈50-kDa CYP2E1 content consistent with structural damage of the protein (Fig. 4*A*). This CYP2E1 loss was prevented by MG262- or epoxomycin-induced proteasomal inhibition (Fig. 4*A*). As expected, this also led to a pronounced accumulation of the ubiquitinated CYP2E1 species (Fig. 4*C*). Cotreatment of rifampin-treated human hepatocytes with the ALD inhibitors 3MA and NH_4Cl for 20 h also led to a significant CYP2E1 stabilization (Fig. 4*B*), with no appreciable

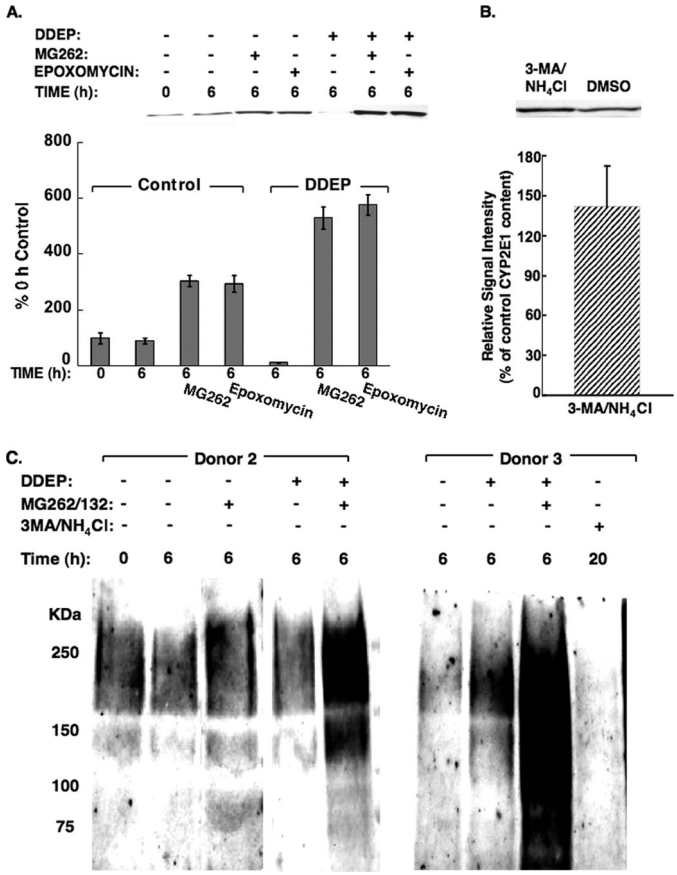

FIGURE 4. **CYP2E1 UPD in cultured human hepatocytes.** Cells from four human donors were treated with rifampin as described previously (see under "Experimental Procedures"). *A,* on day 6, some plates from donor 1 were treated with DDEP (100 μM) for 0–6 h and others with DMSO (vehicle control). Some of these plates with or without DDEP were also treated with the proteasomal inhibitor MG-262 (20 μM) or epoxomycin (10 μM). Cells were harvested and lysates (20 μg of protein) used for CYP2E1 IB analyses (see under "Experimental Procedures") are shown at the *top*. Mean ± S.D. values of three densitometrically quantitated immunoblots from three separate cultures from donor 1 are shown at the *bottom*. *B,* some rifampin-treated cultured hepatocytes from human donor 3 were treated with lysosomal inhibitors 3-MA + NH_4Cl for 20 h as described previously (see under "Experimental Procedures"). A typical immunoblot is shown at the *top* with densitometrically quantitated immunoblots (mean ± S.D.) of three individual lysosomal inhibitor-treated cultures (donor 3) shown at the *bottom*. *C,* CYP2E1 was also immunoprecipitated from lysate aliquots from donor 2 cells treated with MG-262 (supplemental Fig. S1) and donor 3 cells treated with MG-132 or 3-MA + NH_4Cl as described previously in *B* (see under "Experimental Procedures"). The immunoprecipitates from lysates were subjected to IB analyses with a rabbit anti-Ub antibody, as detailed (8, 58). *1st lane* (*extreme left*) corresponds to 0-h controls.

increase in protein ubiquitination in corresponding CYP2E1 immunoprecipitates (Fig. 4*C*). These findings are entirely consistent with the degradation of ubiquitinated CYP2E1 species in the presence of a functional UPS/ERAD.

Analyses of in Vitro CYP2E1 Ubiquitination and the Effects of PKA and/or PKC on This Process—Two E2-E3 complexes have been shown to catalyze P450 ubiquitination *in vitro*: UbcH5a/CHIP in the case of CYP2E1 (22), and both UbcH5a/CHIP and UBC7/gp78 in the case of CYP3A4 (49, 50). To enhance the detection of the ubiquitinated species, P450s were first inactivated by CuOOH *in vitro* before incubation in each of the reconstituted E2/E3 systems. Immunoprecipitation/SDS-PAGE/PhosphorImager/Typhoon-scanning analyses of CYP2E1 incubated for 90 min in an UbcH5a/CHIP-reconstituted ubiquitination system confirmed that it was indeed substantially ubiquitinated (Fig. 5*A*) (22). Inclusion of either PKA or PKC in the incubation greatly enhanced the extent of UbcH5a/CHIP-mediated CYP2E1 ubiquitination (Fig. 5*A*). However, the inclusion of both PKA/PKC in the incubation not only further augmented this CYP2E1 ubiquitination, but the observed CYP2E1 ubiquitination ladder was extended to higher molecular mass levels, indicating that CYP2E1 protein phosphorylation may have enhanced the efficiency and/or extent of its UbcH5a/CHIP-mediated ubiquitination (Fig. 5*A*).

To determine whether UBC7/gp78 was also capable of ubiquitinating CYP2E1, an *in vitro* ubiquitination system reconstituted with this E2-E3 complex was evaluated along with CYP3A4 included in parallel as a positive control (supplemental Fig. S2). Similar immunoprecipitation analyses of each P450 enzyme at 90 min of incubation revealed that UBC7/gp78 was capable of ubiquitinating CYP2E1 and, as reported previously (48, 49), CYP3A4 (Fig. 5*A*; supplemental Fig. S2). The UBC7/gp78-mediated CYP2E1 ubiquitination was found to be not quite as robust as that of CYP3A4 (supplemental Fig. S2). However, inclusion of either PKA or PKC in this incubation system considerably enhanced CYP2E1 ubiquitination (Fig. 5*A*). On the other hand, inclusion of both kinases not only synergized the ubiquitination of CYP2E1 (Fig. 5*A*) but also, as reported earlier (48), that of CYP3A4 (supplemental Fig. S2). These findings thus revealed that CYP2E1 protein phosphorylation substantially enhances its otherwise sluggish ubiquitination by UBC7/gp78.

In Vivo Relevance of PKA-/PKC-mediated Protein Phosphorylation on CYP2E1 UPD/ERAD in Cultured Rat Hepatocytes—Time course analyses of ^{35}S-CYP2E1 immunoprecipitates from control rat hepatocytes by scintillation counting revealed a gradual loss of ^{35}S-CYP2E1 over 4 h following pulse-chase, which was markedly accelerated upon DDEP treatment, as expected (Fig. 5*B*). This DDEP-induced loss was abrogated by concurrent treatment with KT-5720, BisIII, or staurosporine, thereby revealing that each of these kinase inhibitors could block intracellular CYP2E1 turnover, most likely by blocking CYP2E1 phosphorylation and subsequent ubiquitination.

To verify the corresponding effects of each of these kinase inhibitors on intracellular CYP2E1 ubiquitination, the relative fractions of its parent (50 kDa) species and corresponding ubiquitinated high molecular mass (HMM; 65–250 kDa) species in ^{35}S-CYP2E1 immunoprecipitates were evaluated following SDS-PAGE/PhosphorImager/Typhoon-scanning analyses (Fig. 5*C*) as described previously (40). In control (non-DDEP-treated) cells, CYP2E1 was present largely as the parent 50-kDa species with traces of HMM species at time 0 h (Fig. 5*C*). Following DDEP treatment for 2 h, the level of HMM species was increased, apparently at the expense of the parent 50-kDa species (Fig. 5*C*). Treatment of hepatocytes with KT-5720 for 2 h blocked this appearance of HMM-ubiquitinated CYP2E1 species with a corresponding retention of the parent 50-kDa species (Fig. 5*C*). But this KT-5720-induced block somewhat seemed to subside by 4 h (data not shown). Treatment with BisIII for up to 4 h similarly blocked the appearance of HMM-

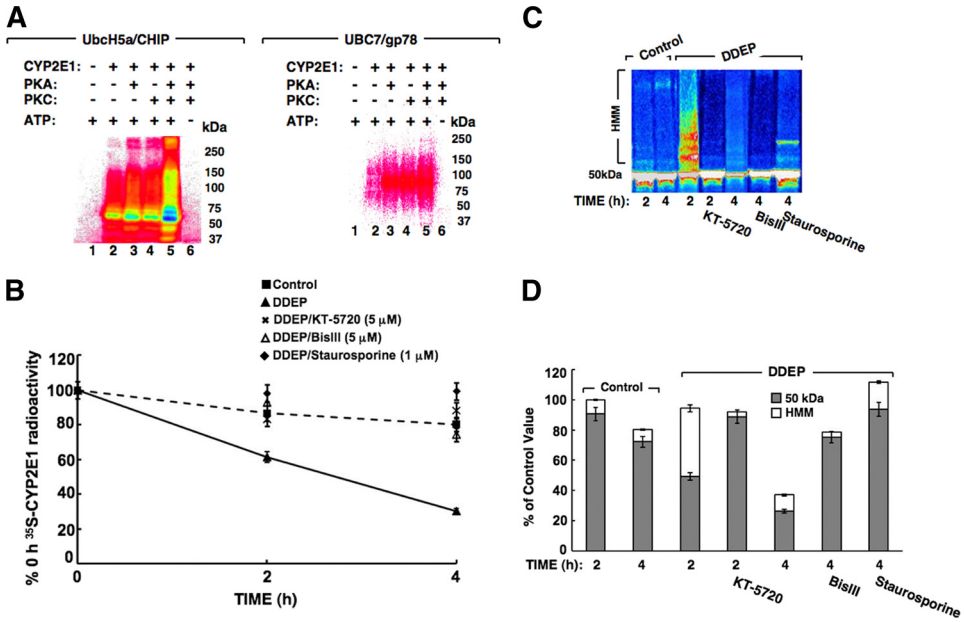

FIGURE 5. **Effects of PKA and/or PKC on CYP2E1 ubiquitination *in vitro* and in cultured rat hepatocytes.** *A,* CYP2E1 ubiquitination in *in vitro* reconstituted E2/E3 systems. PhosphorImager analyses of UbcH5a/CHIP- and UBC7/gp78-mediated ubiquitination of CuOOH-inactivated CYP2E1 in the presence or absence of PKA and/or PKC or in the presence or absence of ATP in the incubation. CYP2E1 was immunoprecipitated from the incubation mixture at 90 min of incubation and subjected to SDS-PAGE analyses. For details of the complete CYP2E1 ubiquitination analyses see under "Experimental Procedures." Data from a typical experiment are depicted. *Lane 1* corresponds to the complete reaction mixture with ATP but no CYP2E1, PKA, or PKC. *Lane 6* corresponds to the complete reaction mixture with CYP2E1 and PKA/PKC but no ATP. Each experiment was conducted in its entirety at the least three separate times. *The color wheel* intensity code is as follows: *black* > *dark blue* > *light blue* > *green* > *yellow* > *orange* > *red*> *magenta* > *white. B,* CYP2E1 ubiquitination and turnover in cultured rat hepatocytes. Cells were subjected to ^{35}S-pulse-chase analyses. At time 0 h of chase, they were treated with DDEP (*solid line*) or DMSO (vehicle; *dashed line*). Thirty min later, they were treated with KT-5720 (5 μM), BisIII (5 μM), staurosporine (1 μM), or DMSO (vehicle). At 0, 2, and 4 h following DDEP, ^{35}S-CYP2E1 was immunoprecipitated from cell lysates. Aliquots of ^{35}S-CYP2E1 immunoprecipitates were subjected to scintillation counting. Values are mean ± S.D. of three individual experiments. *C,* other aliquots of ^{35}S-CYP2E1 immunoprecipitates were subjected to SDS-PAGE and PhosphorImager analyses as described previously. A Typhoon scan of a typical gel is shown. *The color wheel* intensity code is as follows: *white* > *magenta* > *red* > *orange* > *yellow* > *green* > *light blue* > *dark blue* > *black. D,* corresponding quantitation (mean ± S.D.) of the relative intensities of the 50-kDa ^{35}S-CYP2E1 parent species and corresponding HMM-ubiquitinated 65–250-kDa species from three individual experiments (one of which is depicted in *C*) is shown.

ubiquitinated CYP2E1 species with a corresponding retention of the parent 50-kDa species (Fig. 5*C*). This was also true of staurosporine, which tended to retain even more of the CYP2E1 species in its parent form (Fig. 5*C*). The relative quantitation of the HMM ubiquitinated and parent CYP2E1 species from three separate experiments is illustrated (Fig. 5*D*). Together, these findings unequivocally document that inhibition of PKA and/or PKC inhibits intracellular CYP2E1 ubiquitination and consequently its UPD/ERAD.

Identification of Human Liver CYP2E1 Residues Phosphorylated by PKA by LC-MS/MS Analyses—To more completely characterize CYP2E1 phosphorylation, we used LC-MS/MS analyses to identify the sites phosphorylated in the native and CuOOH-inactivated CYP2E1 after their incubation with either PKA or PKC. Ion peaks were selected for MS/MS analyses based on a so-called dynamic exclusion scheme, which selects ions based on a set of criteria such as charge >/ = 2, intensity ranking, and/or whether it has been selected before, etc. Fragmentation spectra were inspected for the presence of a fragment distanced from its parent peptide by 98 Da, a characteristic phosphorylation signature stemming from the elemental loss of phosphoric acid. The manually inspected MS/MS spectra of each phosphorylated peptide indicating the target site are included as evidence (supplemental material). The stoichiometry of phosphorylation at those sites was estimated using a label-free quantification method.[4] *In vitro* incubation of purified recombinant CYP2E1 with PKA predominantly resulted in the phosphorylation of Ser^{129}, as monitored by LC-MS/MS analyses. Semi-quantitative analyses revealed that this phosphorylation constituted 98.2 ± 0.9% of the total phosphorylatable Ser^{129} in the protein, and this extent was not appreciably increased on CuOOH-mediated structural inactivation of the enzyme.[5] However, the phosphorylation of Ser^{145}, Ser^{256}, and Thr^{373} in the native enzyme by PKA was also detected to a minor extent (0.96 ± 0.14, 0.72 ± 0.24, and 1.20 ± 0.05%,

[4] Two strategies were used for the semi-quantitative label-free analysis based on extracted ion chromatograms to estimate the phosphorylation stoichiometry. First, the depletion of the nonphosphorylated peptide was used to estimate the relative quantity of the corresponding phosphorylated peptide. This strategy works well if the nonphosphorylated peptide is detected with good signal to noise ratios in both the control and phosphorylated P450 samples, and the phosphorylation stoichiometry is high (≈ >20%). Second, in the case of low stoichiometry, the intensity of the phosphorylated peptide was used directly. Because the ionization efficiency of the phosphopeptide is typically lower than that of its corresponding nonphosphorylated peptide, its estimation can be significantly under-represented. Thus, in the situation of low stoichiometry, the method may indeed estimate smaller values because the difference in the ionization efficiency between phosphorylated and nonphosphorylated peptides is not known.

[5] In contrast to this native substrate-free CYP2E1 that is very highly phosphorylated by PKA, it is worth noting that substrate-complexed CYP2E1 is apparently more resistant to PKA-mediated phosphorylation (28, 29), which may account for its greater proteolytic stability.

TABLE 1

List of identified PKA-catalyzed CYP2E1 phosphorylation sites

The abbreviations used are as follows: cm, carbamidomethylation; ox, oxidation; p, phosphorylation; RT, peptide retention time. For experimental details, see under "Experimental Procedures." CYP2E1 peptides were derived from Lys-C digests.

No.	Site	Peptide sequence	Mass	z	RT	Expectedvalue	NetPhos score
			m/z		*min*		
1	Ser^{129}	DIRRFpSLTTLRNYGM(ox)GK	531.8	4	26.3	4.9e-3	0.994
		DIRRFpSLTTLRNYGMGK	703.4	3	28.3	4.0e-3	
2	Ser^{145}	Q(Gln→pyroGlu)GNEpSRIQREAHFLLEALRK	615.3	4	28.8	7.3e-4	0.878
3	Ser^{256}	EHHQpSLDPNC(cm)PRDLTDC(cm)LLVEMEK	754.8	4	32.0	6.4e-5	0.105
4	Thr^{373}	DRQEMPYMDAVVHEIQRFITLVPSNLPHEApT RDTIFRGYLIPK	863.6	6	47.9	2.1e-5	0.081

TABLE 2

PKA-mediated phosphorylation, semi-quantitative comparison of native and CuOOH-inactivated CYP2E1

The values are the mean ± S.D. of three individual determinations. - indicates that no phosphorylated peptide was detected in the control sample.

No.	Residue	Control	Native 2E1	CuOOH-2E1
			%	%
1	Ser^{129}	-	98.2 ± 0.92	98.4 ± 0.64
2	Ser^{145}	-	0.96 ± 0.14	1.44 ± 0.07
3	Ser^{256}	-	0.72 ± 0.24	1.10 ± 0.32
4	Thr^{373}	-	1.20 ± 0.05	2.09 ± 0.28

respectively), and similar semi-quantitative analyses indicated that this extent was further increased to 1.44 ± 0.07, 1.10 ± 0.32, and 2.1 ± 0.28%, respectively, upon CuOOH-mediated structural inactivation (Tables 1 and 2; supplemental Figs. S3 and S4).

Identification of Human Liver CYP2E1 Residues Phosphorylated by PKC by LC-MS/MS Analyses—Similar incubation of purified recombinant CYP2E1 with PKC and subsequent LC-MS/MS analyses revealed the phosphorylation of multiple residues in five distinct CYP2E1 domains. The manually inspected MS/MS spectra are provided as evidence (supplemental material). These domains were dissected however into smaller regions of the phosphorylated protein upon Lys-C digestion. The first domain composed of CYP2E1 residues Ser^{56}–Lys^{84} yielded four phosphorylated residues Ser^{56}, Thr^{58}, Thr^{69}, and Ser^{74}. The second CYP2E1 domain composed of residues Glu^{88}–Lys^{160} contained five phosphorylated residues Thr^{121}, Ser^{129}, Thr^{131}, Thr^{132}, and Ser^{145}. The third CYP2E1 domain composed of residues Glu^{244}–Lys^{251} was phosphorylated at Ser^{247} to a minor extent. The fourth domain was composed of Asp^{346}–Lys^{408} containing the predominantly phosphorylated residue Thr^{373}, with Thr^{387} phosphorylated to a lesser extent and Thr^{376} phosphorylated to a minor extent. Finally, the last domain extended from Phe^{421}–Lys^{434}, and contained Ser^{424} and Thr^{432} phosphorylated to a minor extent in the native protein. Of this list, Ser^{56}, Thr^{121}, Ser^{129}, and Thr^{373} are to be underscored as the residues phosphorylated to a major extent by PKC, and this phosphorylation extent was further increased upon inactivation of the enzyme. It is to be noted that Ser^{129}, the residue predominantly phosphorylated by PKA, is also a residue significantly phosphorylated by PKC (23.5 ± 0.45%), and this extent (unlike that with PKA) is further increased to 32.1 ± 0.47% upon CuOOH inactivation. CYP2E1 inactivation also considerably increased the PKC-mediated phosphorylation extent of several residues that were modestly (Thr^{58}, Thr^{69}, Ser^{74}, Thr^{131}, and Thr^{376}), poorly (Ser^{145}, Ser^{424}, and Thr^{432}), or not at all (Thr^{387} and Ser^{431}) detectably phosphorylated in the native protein (Tables 3 and 4; supplemental Figs. S5 and S6).

Identification of Human Liver CYP2E1 Residues Ubiquitinated by UBC7/gp78 or UbcH5a/CHIP by LC-MS/MS Analyses—Protein ubiquitination generally entails the E2/E3-catalyzed covalent attachment of a polyUb chain onto one or more Lys ϵ-NH_2 moieties or the α-N terminus of a suitable substrate. When a ubiquitinated protein is subjected to tryptic/Lys-C digestion, not only is the substrate protein dissected after its unmodified Lys and/or Arg residues but so are the Ub molecules in the polyUb chain, leaving a tell-tale Ub remnant (-GG76 or -LRGG76) covalently attached to its initial site (most frequently a Lys residue) in the substrate-derived tryptic/Lys-C peptide.[6] The corresponding mass signatures of these Ub-derived tags can be conveniently detected by LC-MS/MS analyses through the associated +114.043- or +383.228-Da increase of the modified peptide relative to the unmodified parent peptide (67). Following MS/MS fragmentation of this modified peptide, a characteristic loss of GG- or KGG-associated mass (114.1 or 242.1 Da, respectively) was detected that not only verifies the Ub-derived protein modification but also serves to identify the precise Lys residue ubiquitinated in the protein of interest. Using this approach, we have identified several CYP2E1 residues ubiquitinated by UbcH5a/CHIP and UBC7/gp78 E2/E3 systems in the presence of PKA/PKC (Tables 5 and 6).

Several human liver CYP2E1 peptides containing detectably ubiquitinated Lys residues (Lys^{87}, Lys^{251}, Lys^{275}, and Lys^{410}) were isolated from the UbcH5a/CHIP system (Table 5), and of these, Lys^{251}, Lys^{275}, and Lys^{410} could be verified via LC-MS/MS analyses as ubiquitinated by the diagnostic -GG tag loss (Table 5; supplemental data). The Lys^{251}-ubiquitinated peptide was also found to harbor a phosphorylated residue (Ser^{256}) in its vicinity. Corresponding sites in the orthologous rabbit liver enzyme were also targeted both for phosphorylation and UbcH5a/CHIP-mediated ubiquitination (Table 5; supplemental data). Similarly, several human liver CYP2E1 peptides containing detectably ubiquitinated Lys residues (Lys^{84}, Lys^{87}, Lys^{275}, Lys^{410}, Lys^{420}, Lys^{422}, Lys^{428}, Lys^{434}, and Lys^{461}) were also isolated from the UBC7/gp78 system (Table 6). Of these, Lys^{84}, Lys^{87}, and Lys^{434} could be verified via LC-MS/MS analyses to release the diagnostic -GG tag (Table 6; supplemental data). Lys^{434} was similarly found to be ubiquitinated in the corresponding peptide from the orthologous rabbit liver CYP2E1,

[6] Although in principle the ubiquitination of noncanonical CYP2E1 Ser, Thr, or Cys residues is plausible, they may not have survived the alkaline conditions used for Lys-C/trypsin digestion of the ubiquitinated protein (100–103).

TABLE 3

List of identified PKC-catalyzed CYP2E1 phosphorylation sites

The abbreviations used are as follows: ox, oxidation; p, phosphorylation; RT, peptide retention time. For experimental details, see under "Experimental Procedures." CYP2E1 peptides were derived from Lys-C digests.

No.	Site	Peptide sequence	Mass	*z*	RT	Expected value	NetPhos score
			m/z		*min*		
1	Ser^{56}	pSFTRLAQRFGPVFTLYVGSQRMVVMHGYK	692.0	5	37.8	1.8e-5	0.959
		pSFTRLAQRFGPVFTLYVGSQRMVVMHGYKAVK	626.5	6	35.8	2.0e-4	
2	Thr^{58}	SFpTRLAQRFGPVFTLYVGSQRM(ox)VVMHGYK	695.2	5	35.0	2.8e-6	0.008
3	Thr^{69}	SFTRLAQRFGPVFpTLYVGSQRMVVMHGYK	692.0	5	34.5	7.1e-5	0.496
4	Ser^{74}	SFTRLAQRFGPVFTLYVGpSQRMVVM(ox)HGYK	864.7	4	32.4	1.4e-5	0.050
		SFTRLAQRFGPVFTLYVGpSQRMVVMHGYK	692.0	5	33.7	3.9e-6	
5	Thr^{121}	EALLDYKDEFSGRGDLPAFHAHRDRGIIFNNGPp TWK	1057.5	4	30.4	5.2e-5	0.263
6	Ser^{129}	DIRRFpSLTTLRNYGM(ox)GK	708.7	3	28.0	7.0e-4	0.994
		DIRRFpSLpTTLRNYGMGK	1054.5	2	28.3	5.5e-5	
		DIRRFpSLpTTLRNYGMGK	527.8	4	29.9	4.9e-4	
7	Thr^{131}	DIRRFSLpTTLRNYGMGK	703.4	3	29.9	1.2e-3	0.077
		DIRRFpSLpTTLRNYGMGK	730.0	3	29.5	7.6e-4	
8	Thr^{132}	DIRRFSLTpTLRNYGM(ox)GK	708.69	3	25.8	2.7e-3	0.642
		DIRRFSLTpTLRNYGMGK	527.77	4	28.3	2.1e-4	
9	Ser^{145}	QGNEpSRIQREAHFLLEALRK	619.57	4	31.2	3.4e-3	0.878
10	Ser^{247}	EYVpSERVK	545.25	2	13.6	2.7e-4	0.907
11	Thr^{373}	DRQEMPYMDAVVHEIQRFITLVPSNLPHEApTRDT IFRGYLIPK	863.61	6	48.0	3.0e-6	0.081
		DRQEM(ox)PYMDAVVHEIQRFITLVPSNLPHEApT RDTIFRGYLIPK	1039.3	5	46.0	3.5e-5	
		DRQEM(ox)PYM(ox)DAVVHEIQRFITLVPSNLPHE ApTRDTIFRGYLIPK	1042.5	5	41.5	3.2e-4	
12	Thr^{376}	DRQEM(ox)PYMDAVVHEIQRFITLVPSNLPHEATR DpTIFRGYLIPK	1039.3	5	45.8	4.0e-5	0.877
		DRQEM(ox)PYM(ox)DAVVHEIQRFITLVPSNLPHE ATRDpTIFRGYLIPK	1042.6	5	41.6	2.2e-4	
13	Thr^{387}	GpTVVVPTLDSVLYDNQEFPDPEK	881.41	3	34.2	3.9e-4	0.671
14	Ser^{424}	FKYpSDYFKPFSTGK	897.92	2	30.2	6.3e-7	0.571
15	Ser^{431}	YSDYFKPFpSTGK	507.22	3	26.0	4.9e-5	0.348
16	Thr^{432}	YSDYFKPFSpTGK	760.32	2	27.0	7.2e-6	0.918

TABLE 4

PKC-mediated phosphorylation and semi-quantitative comparison of native and CuOOH-inactivated CYP2E1

The values are the mean ± S.D. of three individual determinations. - indicates that no phosphorylated peptide was detected in the control sample.

No.	Residue	Control	Native 2E1	CuOOH-2E1
			%	%
1	Ser^{56}	-	11.8 ± 0.42	50.8 ± 0.55
2	Thr^{58}	-	4.09 ± 0.29	10.9 ± 0.35
3	Thr^{69}	-	2.59 ± 0.08	4.38 ± 0.12
4	Ser^{74}	-	2.26 ± 0.28	10.9 ± 0.12
5	Thr^{121}	-	35.8 ± 0.38	80.1 ± 0.34
6	Ser^{129}	-	23.5 ± 0.45	32.1 ± 0.47
7	Thr^{131}	-	6.40 ± 0.25	15.3 ± 0.38
8	Thr^{132}	-	3.76 ± 0.13	3.95 ± 0.14
9	Ser^{145}	-	0.14 ± 0.01	0.30 ± 0.01
10	Ser^{247}	-	0.22 ± 0.003	0.28 ± 0.12
11	Thr^{373}	-	39.0 ± 0.54	42.5 ± 0.67
12	Thr^{376}	-	1.72 ± 0.14	2.39 ± 0.23
13	Thr^{387}	-	-	10.3 ± 0.32
14	Ser^{424}	-	0.06 ± 0.002	11.7 ± 0.23
15	Ser^{431}		-	2.49 ± 0.08
16	Thr^{432}		0.76 ± 0.12	1.16 ± 0.08

which also harbored a phosphorylated Ser^{424} (Table 6; supplemental data). Together these findings once again underscore the strong association between P450 protein phosphorylation and ubiquitination irrespective of the particular E2-E3 system employed.

Our LC-MS/MS analyses also enabled us to determine that CYP2E1 polyubiquitination by UbcH5a/CHIP entailed not only Lys^{48}-Ub-Ub linkages, the type of signal associated predominantly with proteasomal targeting, but also Lys^{11}- and Lys^{63}-Ub-Ub linkages (data not shown). However, CYP2E1 ubiquitination by UBC7/gp78 entailed largely a Lys^{48}-Ub-Ub linkage.

DISCUSSION

Despite its relatively poor potential for futile oxidative cycling/catalytic uncoupling, we find that the degradation of heterologously expressed CYP2E1 in yeast still occurs via both ERAD/UPS and ALD pathways as in the mammalian liver. This finding suggests that although such oxidative cycling as proposed previously (41, 42) may significantly influence the targeting of CYP2E1 into mammalian liver UPD pathway, it is by no means the only determinant. CYP2E1 must additionally contain intrinsic "degrons" or post-translationally modified determinants that channel it into this classical ERAD/UPS pathway. Although the precise nature of these CYP2E1 determinants remains to be fully elucidated, it is tempting to speculate that they may include "phosphodegrons" (see below).

In cultured human hepatocytes, this CYP2E1 ERAD/UPS process is not only inhibited by the proteasomal inhibitors but is also enhanced upon DDEP-mediated mechanism-based CYP2E1 inactivation (Fig. 4), consistent with previous reports employing other CYP2E1 suicide inactivators (18–22). Thus, structural inactivation of the enzyme apparently damages the protein, resulting in the exposure of additional degrons or targeting of additional residues for post-translational modification that marks the protein for ERAD/UPS. ALD inhibitors also led to a significant stabilization of CYP2E1 at 20 h of treatment, entirely consistent with the previously noted relatively slower turnover involved in the ALD process (32–38).

Our *in vitro* ubiquitination analyses revealed that of the two specific E2/E3 reconstituted systems examined, UbcH5a/CHIP is indeed relatively more robust than UBC7/gp78 in CYP2E1

TABLE 5

List of identified UbcH5a/CHIP-catalyzed CYP2E1 ubiquitination sites

The abbreviations used are as follows: cm, carbamidomethylation; ox, oxidation; p, phosphorylation. For experimental details, see under "Experimental Procedures." CYP2E1 peptides were derived from Lys-C/tryptic digests.

E2/E3, UbcH5a/CHIP						
No.	Site	Peptide sequence	Mass	z	Expected value	
			m/z			
1	Lys^{275}	Human, DLTDC(cm)LLVEMEK(GG)EK	918.9	2	0.020	
		Rabbit, DFIDSLLIEM(ox)EK(GG)DK	609.3	3	0.010	
		DFIDSLLIEMEK(GG)DK[a]	604.0	3	0.014	
2	Lys^{410}	Human, FK(GG)PEHFLNENGK[a]	525.3	3	0.021	
3	Lys^{251}/Lys^{255}	Human, VK(GG)EHHQpSLDPNC(cm)PR	637.6	3	0.27	
		Rabbit, EHHK(GG)pSLDPSC(cm)PR	414.9	4	0.014	
4	Lys^{87}	Human, AVK(GG)EALLDYK	632.3	2	3.7e-3	
5	Lys^{410}/Lys^{420}	Human, FK(GG)PEHFLNENGK(GG)FK	655.0	3	0.016	
6	Lys^{428}/Lys^{434}	Human, YSDYFK(GG)PFSTGK(GG)R	608.6	3		0.011

[a] Manually annotated spectra are provided as supplemental material.

TABLE 6

List of identified UBC7/gp78-catalyzed CYP2E1 ubiquitination sites

The abbreviations used are as follows: ox, oxidation; p, phosphorylation; cm, carbamidomethylation. For experimental details, see under "Experimental Procedures." CYP2E1 peptides were derived from Lys-C/tryptic digests.

E2/E3,UBC7/gp78					
No.	Site	Peptide sequence	Mass	z	Expected value
			m/z		
1	Lys^{84}	Human, MVVM(ox)HGYK(GG)AVK[a]	696.8	2	0.082
2	Lys^{87}	Human, AVK(GG)EALLDYK[a]	632.4	2	0.052
3	Lys^{434}	Human, YSDYFKPFSTGK(GG)R	570.6	3	0.42
		Rabbit, YSDYFKPFSAGK(GG)R	840.4	2	0.13
		YpSDYFKPFSAGK(GG)R[a]	587.3	3	0.025
4	Lys^{275}	Rabbit, DFIDSLLIEMEK(GG)DK	905.5	2	0.009
5	Lys^{410}/Lys^{420}	Human, FK(GG)PEHFLNENGK(GG)FK	655.0	3	0.046
6	Lys^{422}/Lys^{428}	Human, FK(GG)YSDYFK(GG)PFSTGK	972.0	2	0.071
7	Lys^{461}	Human, MELFLLLC(cm)AILQHFNLK(GG)PLVDPK	956.2	3	0.087

[a] Manually annotated spectra are provided as supplemental material.

ubiquitination, thus confirming the previous finding of Morishima *et al.* (22). However, the inclusion of PKA and/or PKC in the ubiquitination reaction markedly enhanced CYP2E1 ubiquitination by both these E2/E3 systems (Fig. 5*A*). We have previously reported a similar enhancement of UBC7/gp78-mediated CYP3A4 ubiquitination upon its PKA/PKC-mediated phosphorylation (48). More importantly, we now document that such a PKA/PKC-mediated phosphorylation of CYP2E1 may be relevant to its physiological ERAD/UPD. Indeed, treatment of rat hepatocytes with a specific PKA or PKC inhibitor or a general PKA/PKC/PKG inhibitor not only blocked CYP2E1 ubiquitination, but also its turnover (Fig. 5, *B–D*). Collectively, these findings suggest that P450 protein phosphorylation can significantly accelerate the ERAD/UPD of a P450 enzyme by enhancing its ubiquitination. Such enhancement of CYP2E1 ubiquitination, indicated by the greater intensity and extension to higher molecular masses of the ubiquitination profile, may reflect acceleration of the ubiquitination rate, the involvement of a greater number of CYP2E1 residues targeted for ubiquitination, and/or longer polyUb chains appended onto the enzyme.

CYP2E1 contains multiple phosphorylatable residues, in addition to a strategically located PKA RR*X*S[129] recognition motif (28, 51–53, 70–74). Our studies confirm that this Ser^{129} residue is indeed phosphorylated to a very high extent (>98%) by PKA. Although such *in vitro* CYP2E1 phosphorylation by the PKA catalytic subunit may not be physiologically relevant, it is noteworthy that CYP2E1 Ser^{129} residue is also phosphorylated to a lesser albeit significant extent (23.5%) by PKC and liver cytosolic kinases.[7] This PKC-mediated Ser^{129} phosphorylation is further enhanced by CuOOH-mediated structural inactivation of the protein (Table 3). Although such Ser^{129} phosphorylation has been postulated to trigger its rapid proteolytic degradation (28, 29), other CYP2E1 phosphorylatable residues must exist, as mutation of Ser^{129} to Ala or Gly, while retaining enzyme activity, failed to stabilize the enzyme (52).

Indeed, our comprehensive proteomic analyses of the native and CuOOH-inactivated CYP2E1 phosphorylated by either PKA or PKC reveal multisite phosphorylation of the CYP2E1 protein. Accordingly, we identified three new sites (Ser^{145}, Ser^{256}, and Thr^{373}) phosphorylated by PKA along with the previously identified Ser^{129}. Similarly, we identified 14 PKC phosphorylation sites in the native protein, three of which (Ser^{129}, Ser^{145}, and Thr^{373}) were also PKA targets. CYP2E1 structural inactivation not only further enhanced the extent of their phosphorylation but also uncovered two additional sites Ser^{387} and Thr^{431} phosphorylated to a significant extent (Table 3). Inspection of the CYP2E1 crystal structure (71) reveals that many of these residues, particularly those exhibiting the higher phosphorylation extent, are clustered together in distinct patches along the external surface of the protein (Fig. 6). However, additional studies, including site-directed mutagenesis of individual CYP2E1 residues alone and in combination along with the expression/degradation analyses in yeast and/or mammalian cells, will be required to determine the relevance of any specific

[7] Y. Wang and M. A. Correia, unpublished data.

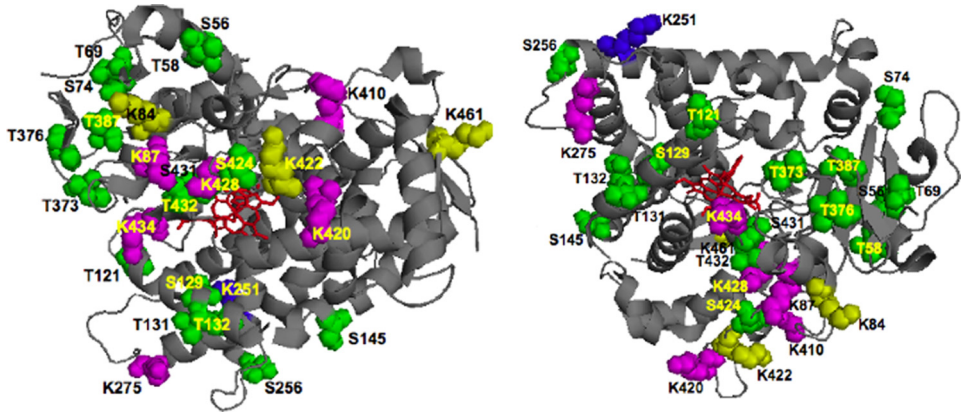

FIGURE 6. **PyMol depiction of CYP2E1 phosphorylation/ubiquitination sites.** Two views of CYP2E1 crystal structure (71) with PKA/PKC-phosphorylated residues identified through LC-MS/MS (>1% relative abundance) shown in *green*, residues ubiquitinated by UBC7/gp78 in *yellow*, that ubiquitinated by UbcH5a/CHIP in *blue*, and those ubiquitinated by both E2-E3 systems in *magenta*.

residue to CYP2E1 ERAD/UPS. Although such analyses may not single out a residue whose phosphorylation is the *sine qua non* of CYP2E1 UPD, it is likely that it will lead to the identification of one or more major determinants or even phosphodegrons. Indeed similar analyses of CYP3A4 have led us to identify Ser^{478} to be just such a major determinant of its ERAD. Ala mutation of this residue significantly impaired CYP3A4 UPD in yeast, and along with those of Ser^{420} and Thr^{264}, it markedly slowed down CYP3A4 UPD in both yeast and mammalian cells (48). Thus, apparently concerted multisite protein phosphorylation can have a synergistic/cooperative influence on P450 ERAD/UPD.

Phosphorylation at two or more sites mediated by one or more cellular kinases is a common feature of many cellular proteins in their UPD recognition and/or targeting (75–86). Phosphorylation of a single phosphorylatable substrate residue by a kinase may be insufficient for its specific recognition by the degradation machinery, but it could serve to "prime" that of another sequentially or spatially related phosphorylatable residue by the same or a different kinase (87). Thus, multisite phosphorylation would not only serve to signal the modified protein as a target for disposal but also control the precise timing of this event by insuring that it is only targeted when all the relevant sites are phosphorylated (88). Several examples exist of multisite phosphorylation on discrete conserved primary sequence peptide motifs known as phosphodegrons that function in the substrate recognition by one or more E3 Ub ligases of the SCF (complex of SKP1, CUL1, and F-box protein) family (88–93). On the other hand, phosphorylated residues dispersed over the entire protein sequence can also serve as "distributed degrons." These act cooperatively in UPD through a highly specific phosphorylation- and sequence-dependent manner, as the recognition of multisite hyperphosphorylated Tau (the pathologic component in Alzheimer disease neurofibrillary tangles) and human androgen receptor by the E3 Ub ligase CHIP complex exemplifies (86, 94–96).[8]

The observed multisite phosphorylation of the CYP2E1 protein, dispersed over the entire length of its primary sequence and contributing to the formation of distinct structural "clusters" on its external surface, may similarly constitute spatially related phosphodegrons that act cooperatively to engage a relevant E2-E3 complex. A similar multisite phosphorylation is also a feature of CYP3A4 ERAD/UPS (48, 97; and our preliminary findings). Thus, it remains to be determined whether such a post-translational modification enhances the molecular interactions of P450 proteins just with a particular E2-E3 complex, as our findings seem to indicate, or additionally with the other critical ERAD participants along the P450 degradation trail.

Our findings also reveal multisite ubiquitination of human liver CYP2E1 (Fig. 6), a protein studded with 29 Lys residues,[6] most of them solvent-accessible (70, 71). It has been previously proposed on the basis of a CYP2E1 homology model that two Lys residues (Lys^{317} and Lys^{324}) in an evolutionarily highly conserved CYP2E1 Lys^{317}–Ala^{340} domain were ubiquitinated by the rabbit reticulocyte ubiquitination machinery (98). From CYP2E1 molecular modeling analyses, these Lys residues were predicted to be cytosolically accessible. Indeed, a specific antibody raised against this domain was shown not only to inhibit rat liver microsomal CYP2E1 catalytic activity but also CYP2E1 ubiquitination (98). Our LC-MS/MS analyses of human and rabbit liver CYP2E1 ubiquitination identified several Lys residues (Lys^{84}, Lys^{87}, and Lys^{251} (human); Lys^{255} (rabbit); Lys^{275}, Lys^{410}, Lys^{420}, Lys^{422}, Lys^{428}, Lys^{434}, and Lys^{461}) in both human and rabbit liver CYP2E1 proteins as targets of both UbcH5a/CHIP and UBC7/gp78 (Tables 5 and 6). Of these, Lys^{84}, Lys^{87}, Lys^{251}/Lys^{255}, Lys^{275}, Lys^{410}, and Lys^{434} were conclusively verified by LC-MS/MS analyses to contain the diagnostic ubiquitination tag (Tables 5 and 6). Although UBC7/gp78 favored some CYP2E1 residues (Lys^{84}, Lys^{422}, and Lys^{461}) and UbcH5a/CHIP others (Lys^{251}/Lys^{255}), there was considerable overlap (Lys^{87}, Lys^{275}, Lys^{410}, Lys^{420}, Lys^{428}, and Lys^{434}), thereby revealing that although each E2-E3 complex has some preferred target sites, their interactions with a particular CYP2E1 domain were not mutually exclusive. Furthermore, inspection of the CYP2E1 crystal structure reveals that several of the ubiquitinated CYP2E1 Lys residues were in close vicinity of its phosphorylated clusters (Fig. 6), thus reinforcing the notion that phosphorylation of a P450 domain may indeed serve to engage the E2-E3 complex for its ubiquitination.

[8] UPD of the forkhead transcription factor FoxO1 also involves its Akt-mediated phosphorylation on Ser^{256} for its recognition by the UbcH5a-CHIP complex. It is unclear whether phosphorylation of additional sites is involved (96).

In summary, our findings of hepatic CYP2E1 degradation herein confirm yet again that the pathways of P450 ERAD/UPS and ALD are evolutionarily highly conserved from yeast to man. In common with that of CYP3A4, CYP2E1 ERAD/UPS apparently also involves post-translational protein phosphorylation by cellular kinases and ubiquitination by both UbcH5a/CHIP and UBC7/gp78 E2-E3 complexes. Although P450 protein phosphorylation apparently precedes ubiquitination (Fig. 5) (48), it is unclear whether *in vivo* the two E2-E3 systems act concertedly, concurrently, or even sequentially. Nevertheless, although multiple Lys residues are ubiquitinated, and it is unknown whether ubiquitination of any specific CYP2E1 Lys residue is critical to its ERAD/UPS, the predominant appendage of Lys[48] Ub-Ub-linkages suggests that the primary role of such protein polyubiquitination is to target P450s to ERAD/UPS.

Acknowledgments—We sincerely thank Dr. Todd Porter (University of Kentucky, Lexington) for the human CYP2E1 cDNA and Drs. Randy Hampton (University of California, San Diego) and Mark Hochstrasser (Yale University) for the yeast strains; Dr. A. M. Weissman (NCI, National Institutes of Health) for the UBC7 and gp78C expression plasmids; Dr. Cam Patterson (University of North Carolina) for the CHIP expression plasmid; Dr. Lucy Waskell (University of Michigan) for the b_5 expression plasmid; and Dr. Charles Kasper (University of Wisconsin) for the OR expression plasmid. We also thank Dr. Ed LeCluyse and Rachel Whisnant (CellzDirect, Invitrogen) for the human hepatocytes, and Chris Her (University of California, San Francisco, Liver Center Cell and Tissue Biology Core Facility; Dr. J. J. Maher, Director) for rat hepatocyte isolation. We also acknowledge the University of California, San Francisco, Liver Center Core on Cell and Tissue Biology, supported by National Institutes of Health Grant P30DK26743 from NIDDK.

REFERENCES

1. Guengerich, F. P. (2005) *Cytochrome P450: Structure, Mechanism, and Biochemistry* (Ortiz de Montellano, P., ed) 3rd Ed., pp. 377–530, Kluwer-Academic/Plenum Press, New York
2. Correia, M. A. (2005) *Cytochrome P450: Structure, Mechanism, and Biochemistry* (Ortiz de Montellano, P., ed) 3rd Ed., pp. 619–657, Kluwer-Academic/Plenum Press. New York
3. Watkins, P. B., Wrighton, S. A., Schuetz, E. G., Maurel, P., and Guzelian, P. S. (1986) *J. Biol. Chem.* **261,** 6264–6271
4. Song, B. J., Veech, R. L., Park, S. S., Gelboin, H. V., and Gonzalez, F. J. (1989) *J. Biol. Chem.* **264,** 3568–3572
5. Roberts, B. J., Song, B. J., Soh, Y., Park, S. S., and Shoaf, S. E. (1995) *J. Biol. Chem.* **270,** 29632–29635
6. Correia, M. A. (1991) *Methods Enzymol.* **206,** 315–325
7. Correia, M. A. (2003) *Drug Metab. Rev.* **35,** 107–143
8. Correia, M. A., Sadeghi, S., and Mundo-Paredes, E. (2005) *Annu. Rev. Pharmacol. Toxicol.* **45,** 439–464
9. Correia, M. A., and Liao, M. (2007) *Expert Opin. Drug Metab. Toxicol.* **3,** 33–49
10. Lown, K. S., Bailey, D. G., Fontana, R. J., Janardan, S. K., Adair, C. H., Fortlage, L. A., Brown, M. B., Guo, W., and Watkins, P. B. (1997) *J. Clin. Invest.* **99,** 2545–2553
11. Paine, M. F., Widmer, W. W., Hart, H. L., Pusek, S. N., Beavers, K. L., Criss, A. B., Brown, S. S., Thomas, B. F., and Watkins, P. B. (2006) *Am. J. Clin. Nutr.* **83,** 1097–1105
12. Correia, M. A., Decker, C., Sugiyama, K., Caldera, P., Bornheim, L., Wrighton, S. A., Rettie, A. E., and Trager, W. F. (1987) *Arch. Biochem. Biophys.* **258,** 436–451
13. Correia, M. A., Davoll, S. H., Wrighton, S. A., and Thomas, P. E. (1992) *Arch. Biochem. Biophys.* **297,** 228–238
14. Korsmeyer, K. K., Davoll, S., Figueiredo-Pereira, M. E., and Correia, M. A. (1999) *Arch. Biochem. Biophys.* **365,** 31–44
15. Wang, H. F., Figueiredo Pereira, M. E., and Correia, M. A. (1999) *Arch. Biochem. Biophys.* **365,** 45–53
16. Faouzi, S., Medzihradszky, K. F., Hefner, C., Maher, J. J., and Correia, M. A. (2007) *Biochemistry* **46,** 7793–7803
17. Correia M. A., and Ortiz de Montellano, P. R. (2005) *Cytochrome P450: Structure, Mechanism, and Biochemistry* (Ortiz de Montellano, P., ed) 3rd Ed., pp. 247–322, Kluwer-Academic/Plenum Press, New York
18. Tierney, D. J., Haas, A. L., and Koop, D. R. (1992) *Arch. Biochem. Biophys.* **293,** 9–16
19. Sohn, D. H., Yun, Y. P., Park, K. S., Veech, R. L., and Song, B. J. (1991) *Biochem. Biophys. Res. Commun.* **179,** 449–454
20. Yang, M. X., and Cederbaum, A. I. (1997) *Arch. Biochem. Biophys.* **341,** 25–33
21. Huan, J. Y., Streicher, J. M., Bleyle, L. A., and Koop, D. R. (2004) *Toxicol. Appl. Pharmacol.* **199,** 332–343
22. Morishima, Y., Peng, H. M., Lin, H. L., Hollenberg, P. F., Sunahara, R. K., Osawa, Y., and Pratt, W. B. (2005) *Biochemistry* **44,** 16333–16340
23. Lee, C. M., Kim, B. Y., Li, L., and Morgan, E. T. (2008) *J. Biol. Chem.* **283,** 889–898
24. Chien, J. Y., Thummel, K. E., and Slattery, J. T. (1997) *Drug Metab. Dispos.* **25,** 1165–1175
25. Yang, J., Liao, M., Shou, M., Jamei, M., Yeo, K. R., Tucker, G. T., and Rostami-Hodjegan, A. (2008) *Curr. Drug Metab.* **9,** 384–394
26. Kalgutkar, A. S., Obach, R. S., and Maurer, T. S. (2007) *Curr. Drug Metab.* **8,** 407–447
27. Xu, L., Chen, Y., Pan, Y., Skiles, G. L., and Shou, M. (2009) *Drug Metab. Dispos.* **37,** 2330–2339
28. Eliasson, E., Johansson, I., and Ingelman-Sundberg, M. (1990) *Proc. Natl. Acad. Sci. U.S.A.* **87,** 3225–3229
29. Eliasson, E., Mkrtchian, S., and Ingelman-Sundberg, M. (1992) *J. Biol. Chem.* **267,** 15765–15769
30. Zhukov, A., Werlinder, V., and Ingelman-Sundberg, M. (1993) *Biochem. Biophys. Res. Commun.* **197,** 221–228
31. Goasduff, T., and Cederbaum, A. I. (2000) *Arch. Biochem. Biophys.* **379,** 321–330
32. Roberts, B. J. (1997) *J. Biol. Chem.* **272,** 9771–9778
33. Masaki, R., Yamamoto, A., and Tashiro, Y. (1987) *J. Cell Biol.* **104,** 1207–1215
34. Ronis, M. J., Johansson, I., Hultenby, K., Lagercrantz, J., Glaumann, H., and Ingelman-Sundberg, M. (1991) *Eur. J. Biochem.* **198,** 383–389
35. Murray, B. P., Zgoda, V. G., and Correia, M. A. (2002) *Mol. Pharmacol.* **61,** 1146–1153
36. Liao, M., Zgoda, V. G., Zgoda, V. A., Murray, B. P., and Correia, M. A. (2005) *Mol. Pharmacol.* **67,** 1460–1469
37. Bardag-Gorce, F., Li, J., French, B. A., and French, S. W. (2002) *Free Radic. Biol. Med.* **32,** 17–21
38. Bardag-Gorce, F., French, B. A., Nan, L., Song, H., Nguyen, S. K., Yong, H., Dede, J., and French, S. W. (2006) *Exp. Mol. Pathol.* **81,** 191–201
39. Liao, M., Faouzi, S., Karyakin, A., and Correia, M. A. (2006) *Mol. Pharmacol.* **69,** 1897–1904
40. Acharya, P., Liao, M., Engel, J. C., and Correia, M. A. (2011) *J. Biol. Chem.* **286,** 3815–3828
41. Zhukov, A., and Ingelman-Sundberg, M. (1999) *Biochem. J.* **340,** 453–458
42. Goasduff, T., and Cederbaum, A. I. (1999) *Arch. Biochem. Biophys.* **370,** 258–270
43. Hampton, R. Y., Gardner, R. G., and Rine, J. (1996) *Mol. Biol. Cell* **7,** 2029–2044
44. Huyer, G., Piluek, W. F., Fansler, Z., Kreft, S. G., Hochstrasser, M., Brodsky, J. L., and Michaelis, S. (2004) *J. Biol. Chem.* **279,** 38369–38378
45. Swanson, R., Locher, M., and Hochstrasser, M. (2001) *Genes Dev.* **15,** 2660–2674
46. Pompon, D., Louerat, B., Bronine, A., and Urban, P. (1996) *Methods Enzymol.* **272,** 51–64

47. Kostova, Z., Tsai, Y. C., and Weissman, A. M. (2007) *Semin. Cell Dev. Biol.* **18,** 770–779
48. Wang, Y., Liao, M., Hoe, N., Acharya, P., Deng, C., Krutchinsky, A. N., and Correia, M. A. (2009) *J. Biol. Chem.* **284,** 5671–5684
49. Pabarcus, M. K., Hoe, N., Sadeghi, S., Patterson, C., Wiertz, E., and Correia, M. A. (2009) *Arch. Biochem. Biophys.* **483,** 66–74
50. Kim, S. M., Acharya, P., Engel, J. C., and Correia, M. A. (2010) *J. Biol. Chem.* **285,** 35866–35877
51. Pyerin, W., and Taniguchi, H. (1989) *EMBO J.* **8,** 3003–3010
52. Freeman, J. E., and Wolf, C. R. (1994) *Biochemistry* **33,** 13963–13966
53. Redlich, G., Zanger, U. M., Riedmaier, S., Bache, N., Giessing, A. B., Eisenacher, M., Stephan, C., Meyer, H. E., Jensen, O. N., and Marcus, K. (2008) *J. Proteome Res.* **7,** 4678–4688
54. Huan, J. Y., and Koop, D. R. (1999) *Drug Metab. Dispos.* **27,** 549–554
55. Pearce, R. E., Lu, W., Wang, Y., Uetrecht, J. P., Correia, M. A., and Leeder, J. S. (2008) *Drug Metab. Dispos.* **36,** 1637–1649
56. Koop, D. R., and Coon, M. J. (1984) *Mol. Pharmacol.* **25,** 494–501
57. Masimirembwa, C. M., Otter, C., Berg, M., Jönsson, M., Leidvik, B., Jonsson, E., Johansson, T., Bäckman, A., Edlund, A., and Andersson, T. B. (1999) *Drug Metab. Dispos.* **27,** 1117–1122
58. Acharya, P., Engel, J. C., and Correia, M. A. (2009) *Mol. Pharmacol.* **76,** 503–515
59. Acharya, P., Chen, J. J., and Correia, M. A. (2010) *Mol. Pharmacol.* **77,** 575–592
60. Hewitt, N. J., Lechón, M. J., Houston, J. B., Hallifax, D., Brown, H. S., Maurel, P., Kenna, J. G., Gustavsson, L., Lohmann, C., Skonberg, C., Guillouzo, A., Tuschl, G., Li, A. P., LeCluyse, E., Groothuis, G. M., and Hengstler, J. G. (2007) *Drug Metab. Rev.* **39,** 159–234
61. Chalkley, R. J., Baker, P. R., Medzihradszky, K. F., Lynn, A. J., and Burlingame, A. L. (2008) *Mol. Cell. Proteomics* **7,** 2386–2398
62. Clauser, K. R., Baker, P., and Burlingame, A. L. (1999) *Anal. Chem.* **71,** 2871–2882
63. Balgley, B. M., Laudeman, T., Yang, L., Song, T., and Lee, C. S. (2007) *Mol. Cell. Proteomics* **6,** 1599–1608
64. Ficarro, S. B., McCleland, M. L., Stukenberg, P. T., Burke, D. J., Ross, M. M., Shabanowitz, J., Hunt, D. F., and White, F. M. (2002) *Nat. Biotechnol.* **20,** 301–305
65. Steen, H., Jebanathirajah, J. A., Springer, M., and Kirschner, M. W. (2005) *Proc. Natl. Acad. Sci. U.S.A.* **102,** 3948–3953
66. Steen, J. A., Steen, H., Georgi, A., Parker, K., Springer, M., Kirchner, M., Hamprecht, F., and Kirschner, M. W. (2008) *Proc. Natl. Acad. Sci. U.S.A.* **105,** 6069–6074
67. Peng, J., Schwartz, D., Elias, J. E., Thoreen, C. C., Cheng, D., Marsischky, G., Roelofs, J., Finley, D., and Gygi, S. P. (2003) *Nat. Biotechnol.* **21,** 921–926
68. Kikkert, M., Doolman, R., Dai, M., Avner, R., Hassink, G., van Voorden, S., Thanedar, S., Roitelman, J., Chau, V., and Wiertz, E. (2004) *J. Biol. Chem.* **279,** 3525–3534
69. Fang, S., Ferrone, M., Yang, C., Jensen, J. P., Tiwari, S., and Weissman, A. M. (2001) *Proc. Natl. Acad. Sci. U.S.A.* **98,** 14422–14427
70. Umeno, M., McBride, O. W., Yang, C. S., Gelboin, H. V., and Gonzalez, F. J. (1988) *Biochemistry* **27,** 9006–9013
71. Porubsky, P. R., Meneely, K. M., and Scott, E. E. (2008) *J. Biol. Chem.* **283,** 33698–33707
72. Menez, J. F., Machu, T. K., Song, B. J., Browning, M. D., and Deitrich, R. A. (1993) *Alcohol Alcohol.* **28,** 445–451
73. Aguiar, M., Masse, R., and Gibbs, B. F. (2005) *Drug Metab. Rev.* **37,** 379–404
74. Oesch-Bartlomowicz, B., and Oesch, F. (2005) *Biochem. Biophys. Res. Commun.* **338,** 446–449
75. Willems, A. R., Lanker, S., Patton, E. E., Craig, K. L., Nason, T. F., Mathias, N., Kobayashi, R., Wittenberg, C., and Tyers, M. (1996) *Cell* **86,** 453–463
76. Kaplan, K. B., Hyman, A. A., and Sorger, P. K. (1997) *Cell* **91,** 491–500
77. Butler, M. P., Hanly, J. A., and Moynagh, P. N. (2007) *J. Biol. Chem.* **282,** 29729–29737
78. Feldman, R. M., Correll, C. C., Kaplan, K. B., and Deshaies, R. J. (1997) *Cell* **91,** 221–230
79. Verma, R., Annan, R. S., Huddleston, M. J., Carr, S. A., Reynard, G., and Deshaies, R. J. (1997) *Science* **278,** 455–460
80. Miyamoto, S., Maki, M., Schmitt, M. J., Hatanaka, M., and Verma, I. M. (1994) *Proc. Natl. Acad. Sci. U.S.A.* **91,** 12740–12744
81. Brown, K., Gerstberger, S., Carlson, L., Franzoso, G., and Siebenlist, U. (1995) *Science* **267,** 1485–1488
82. Chen, Z., Hagler, J., Palombella, V. J., Melandri, F., Scherer, D., Ballard, D., and Maniatis, T. (1995) *Genes Dev.* **9,** 1586–1597
83. Chen, Z. J., Parent, L., and Maniatis, T. (1996) *Cell* **84,** 853–862
84. Dai, R. M., Chen, E., Longo, D. L., Gorbea, C. M., and Li, C. C. (1998) *J. Biol. Chem.* **273,** 3562–3573
85. Miranda, M., Wu, C. C., Sorkina, T., Korstjens, D. R., and Sorkin, A. (2005) *J. Biol. Chem.* **280,** 35617–35624
86. Shimura, H., Schwartz, D., Gygi, S. P., and Kosik, K. S. (2004) *J. Biol. Chem.* **279,** 4869–4876
87. Cohen, P. (2000) *Trends Biochem. Sci.* **25,** 596–601
88. Ang, X. L., and Wade Harper, J. (2005) *Oncogene* **24,** 2860–2870
89. Reed, S. I. (2006) *Results Probl. Cell Differ.* **42,** 147–181
90. Welcker, M., and Clurman, B. E. (2008) *Nat. Rev. Cancer* **8,** 83–93
91. Olson, B. L., Hock, M. B., Ekholm-Reed, S., Wohlschlegel, J. A., Dev, K. K., Kralli, A., and Reed, S. I. (2008) *Genes Dev.* **22,** 252–264
92. Olsen, B. B., and Guerra, B. (2008) *Mol. Cell. Biochem.* **316,** 115–126
93. Klotz, K., Cepeda, D., Tan, Y., Sun, D., Sangfelt, O., and Spruck, C. (2009) *Exp. Cell Res.* **315,** 1832–1839
94. Cripps, D., Thomas, S. N., Jeng, Y., Yang, F., Davies, P., and Yang, A. J. (2006) *J. Biol. Chem.* **281,** 10825–10838
95. Dickey, C. A., Kamal, A., Lundgren, K., Klosak, N., Bailey, R. M., Dunmore, J., Ash, P., Shoraka, S., Zlatkovic, J., Eckman, C. B., Patterson, C., Dickson, D. W., Nahman, N. S., Jr., Hutton, M., Burrows, F., and Petrucelli, L. (2007) *J. Clin. Invest.* **117,** 648–658
96. Rees, I., Lee, S., Kim, H., and Tsai, F. T. (2006) *Biochim. Biophys. Acta* **1764,** 1073–1079
97. Wang, X., Medzihradszky, K. F., Maltby, D., and Correia, M. A. (2001) *Biochemistry* **40,** 11318–11326
98. Banerjee, A., Kocarek, T. A., and Novak, R. F. (2000) *Drug Metab. Dispos.* **28,** 118–124
99. He, K., Bornheim, L. M., Falick, A. M., Maltby, D., Yin, H., and Correia, M. A. (1998) *Biochemistry* **37,** 17448–17457
100. Li, F., Xie, P., Fan, Y., Zhang, H., Zheng, L., Gu, D., Patterson, C., and Li, H. (2009) *J. Biol. Chem.* **284,** 20090–20098
101. Wang, X., Herr, R. A., Chua, W. J., Lybarger, L., Wiertz, E. J., and Hansen, T. H. (2007) *J. Cell Biol.* **177,** 613–624
102. Cadwell, K., and Coscoy, L. (2005) *Science* **309,** 127–130
103. Ishikura, S., Weissman, A. M., and Bonifacino, J. S. (2010) *J. Biol. Chem.* **285,** 23916–23924